Environmental Science Advances

ROYAL SOCIETY OF CHEMISTRY

PAPER

View Article Online
View Journal | View Issue

Cite this: *Environ. Sci.: Adv.*, 2025, **4**, 469

Nanocomposite UF membrane of PVC/nano-silica modified with SDS for carwash wastewater treatment

Eman S. A. Al-Sammarraie,[ab] T. M. Sabirova,[a] Hicham Meskher, *[c] Raed A. Al-Juboori, [de] Grigory V. Zyryanov[af] and Qusay F. Alsalhy*[g]

This study presents an investigation of a novel fouling-resistant mixed matrix membrane (MMM) composed of ultrafiltration PVC incorporating silica nanoparticles modified with sodium dodecyl sulfate (SiO_2-SDS) for carwash wastewater treatment. The hydrophilic SiO_2-SDS was synthesized by modifying SDS molecules onto the surfaces of silica nanoparticles (SiO_2 NPs). Later, SiO_2-SDS NPs were incorporated into a PVC polymeric matrix at an optimized ratio. The prepared virgin membrane and MMMs were characterized using Fourier transform infrared spectroscopy (FTIR), scanning electron microscopy-energy dispersive X-ray (SEM-EDX) spectroscopy, and atomic force microscopy (AFM). The results revealed that MMMs prepared with 0.15 wt% SiO_2-SDS NPs exhibited optimum characteristics and performance, where the highest thickness of 118.71 ± 0.42 μm and maximum porosity of 81.40 ± 0.23% were obtained. The pure water flux of this membrane reached 127.75 ± 1.72 L m^{-2} h^{-1}, which is better than that of other modified membranes. This membrane achieved high removal of total suspended solids and chemical oxygen demand of 93% and 78%, respectively, when used with real carwash wastewater. Additionally, the 0.15 wt% SiO_2-SDS NPs exhibited stable performance during prolonged operation, resulting in the best flux recovery ratio of 80% among other tested membranes, signifying its superior fouling resistance bestowed by the hydrophilic nature of the incorporated SiO_2-SDS NPs.

Received 21st March 2024
Accepted 30th November 2024

DOI: 10.1039/d4va00088a

rsc.li/esadvances

Environmental significance

Carwash wastewater is produced in large quantities worldwide. The pollutants present in this wastewater are harmful to the environment, such as elevated chemical oxygen demand (COD). Additionally, sending this wastewater to municipal wastewater treatment facilities can pose technical problems, such as foaming. Ultrafiltration (UF) can be used for effective carwash wastewater treatment and possible reuse; however, it is rapidly fouled when used with this type of wastewater. Hence, this study proposes incorporating modified silica nanoparticles with sodium dodecyl sulfate (SiO_2-SDS) into a polyvinyl chloride (PVC) membrane to improve the antifouling properties of the latter. The optimum percentage of SiO_2-SDS resulted in a flux recovery of 80% with high COD removal.

1. Introduction

Over the last decades, global water scarcity has risen dramatically due to the geographic mismatch between the demand for and availability of freshwater. Additionally, access to freshwater and its sources is considered a serious challenge in several areas worldwide.[1,2] Rapid population growth, global warming, and the environmental impact of industrialization have made the situation more complicated. To improve the present situation, the introduction of novel cost-effective and eco-friendly water treatment technologies is urgently needed to meet the needs of this demographic and industrial growth.[3,4]

Membrane-based techniques are considered a typical example of eco-friendly water purification processes, which are used in desalination and other applications, including but not limited to the treatment of industrial wastewater from pharmaceuticals manufacturing and agro-alimentary industries,

[a]*Department of Chemical Technology of Fuel and Industrial Ecology, Institute of Chemical Technology, Ural Federal University Named After First President of Russia B.N. Yeltsin, Mira Street 19, 620002 Yekaterinburg, Russia*

[b]*Environmental Research Center, University of Technology-Iraq, 10066 Baghdad, Iraq*

[c]*Division of Process Engineering, College of Science and Technology, Chadli Bendjedid University, 36000, Algeria. E-mail: h.meskher@univ-eltarf.dz*

[d]*NYUAD Water Research Center, New York University Abu Dhabi, P.O. Box 129188, Abu Dhabi, United Arab Emirates*

[e]*Water and Environmental Engineering Research Group, Department of Built Environment, Aalto University, P. O. Box 15200, Aalto, FI-00076, Espoo, Finland. E-mail: Raed.Al-Juboori@Aalto.fi*

[f]*Postovsky Institute of Organic Synthesis, Ural Division of the Russian Academy of Sciences, Yekaterinburg, 620137, Russia*

[g]*Membrane Technology Research Unit, Department of Chemical Engineering, University of Technology-Iraq, Alsinaa Street 52, 10066 Baghdad, Iraq. E-mail: qusay.f.abdulhameed@uotechnology.edu.iq*

and waste from nuclear processes.[5,6] Abbas T. K. *et al.*,[7] created a unique NaY-zeolite-modified polyethersulfone (PES) membrane for the removal of ^{137}Cs from actual nuclear liquid waste. A membrane prepared with 0.15% NaY exhibited the best removal rate (90.2%), which increased to 99.2% when copper ferrocyanide (CuFC), a ligand agent, was added to the feed solution to increase the removal efficiency. However, membranes often face the serious issue of fouling, which has a negative impact on the performance of the membrane, which could be reflected in the permeate quantity and quality.[8–10] Membrane fouling depends basically on the type and concentration of the feed and also on the operating conditions and membrane surface characteristics.[3,11,12] Therefore, modifications to membrane surface chemistry could be considered to solve this issue by improving the surface hydrophilic properties of the membrane surface and mitigating its fouling through specific chemical or/and physical routes.[13–15] Several techniques have been introduced to modify membrane surfaces, such as dip coating and blending, where a host polymer is blended with a hydrophilic inorganic nanomaterial such as alumina, zinc, or silica.[11,16–18] Unfortunately, the up-scaling of this technique is complicated due to the weak interaction between the host polymer and the inorganic nanomaterials, which limits blending for commercial applications.[19,20] In addition, material agglomeration and leaching out from the membrane matrix often occur during the process, which may ruin the membrane and worsen its performance during the process of water treatment or desalination.[21,22] Therefore, a simpler and more effective method is very desirable.

In this context, several polymers have been used in membrane surface modification to improve their fouling resistance.[23–25] Incorporating polyvinyl chloride (PVC) into a membrane structure has exhibited outstanding performance, especially for water desalination.[26] Among the characteristics that distinguish PVC from most polymers is its relatively low cost, outstanding physicochemical properties and excellent thermal stability.[27,28] Once modified with PVC, the membrane becomes more resistant to fouling, more stable and exhibits better separation performance. The most important drawback of PVC is its hydrophobicity, which is likely to result in more fouling during filtration.[29] To resolve this problem, Alsalhy *et al.*,[30] reported the successful embedding of ZnO NPs as an anti-fouling agent on a PVC membrane to investigate the removal of chemical oxygen demand. The successful embedding of ZnO NPs on PVC membranes improved their permeability by up to 325% and boosted their long-term process from 29 to 70 days before membrane cleaning.[30] Silica nanoparticles (SiO_2 NPs) could also be used as an option to improve membrane performance due to their low cost, ease of preparation, excellent stability, and hydrophilicity. Several studies have reported the successful use of SiO_2 NPs as membrane fillers and pore-forming agents, whereas other work has highlighted their potential to improve membrane hydrophilicity and antifouling properties without affecting membrane structure or morphology.[31–34] Al-Araji *et al.*,[35] developed a novel nanocomposite ultrafiltration membrane based on PEI-modified silica nanoparticles for treating textile wastewater. A denser structural membrane with slightly broader pore size, showing the best removal performance, notable antifouling characteristics, and stability over an extended period of operation were demonstrated by a nanocomposite membrane that was generated with the highest ratio of nanoadditives (0.7 wt%).[35] However, the content of SiO_2 NPs used should be optimized to ensure efficient performance. A low-cost nano-SiO_2/PVC-based-membrane was fabricated by Z. Yu *et al.*,[36] to investigate its potential in wastewater treatment. After optimization of SiO_2 content, the fabricated membrane exhibited outstanding hydrophilicity, mechanical properties, and improved pure water flux. However, the nano-SiO_2/PVC based-membrane suffered from high viscosity levels, an unfavorable degassing effect, and film-formation performance once the content of SiO_2 was 3 wt% or more.[36] This was also confirmed by Saberi *et al.*,[37] who reported that increasing the SiO_2 NP content beyond 3.5 wt% decreased the membrane performance because of agglomeration of the nanoparticles and pore blockage.[37]

This study proposes the use of silica-sodium dodecyl sulfate nanoparticles (SiO_2-SDS NPs) for modifying the structural properties of a PVC membrane to improve its performance and antifouling properties, which has not been explored in previous studies. Modified silica-sodium dodecyl sulfate nanoparticles (SiO_2-SDS NPs) of various concentrations were incorporated into the PVC doping solutions. Subsequently, the solutions were cast into flat-sheet membranes employing the classical phase-inversion technique. The resulting membranes were then characterized using X-ray diffraction (XRD), scanning electron microscopy (SEM), atomic force microscopy (AFM), and Fourier transform infrared spectroscopy (FTIR), to observe the influence of SiO_2-SDS nanoparticles on the morphology of the membranes. Furthermore, the separation performance of the ultrafiltration membranes was determined through measurement of pure water flux and real carwash wastewater rejection. Finally, fouling experiments were performed to evaluate the flux recovery ratio for the pristine membrane and MMMs.

2. Experimental

2.1. Materials

PVC polymer (average $M_w = 65\,000$ g mol^{-1}) was acquired from Georgia Gulf Co. *N*,*N* dimethyl acetamide (DMAc) was purchased from Sigma-Aldrich Co. SiO_2 NPs with a specific surface area of ~640 m^2 g^{-1} and an average particle size of 15–20 nm were obtained from US Research Nanomaterials Inc., USA. Sodium dodecyl sulfate (SDS) with a molar mass of 288.372 g mol^{-1} was acquired from Central Drug House, India.

2.2. Modification process of SiO_2 NPs with SDS

The SiO_2-SDS nanoparticles were prepared by wet chemical synthesis.[38] The silica nanoparticles were added to 500 ml of deionized water and mixed well under continuous stirring for about 10 min and then heated to 80 °C. A 5% SDS was added to the above silica suspension solution and stirred for about 1 h. NaOH solution (1.5 ml) was added dropwise to the mixture solution for precipitation and the pH was maintained between

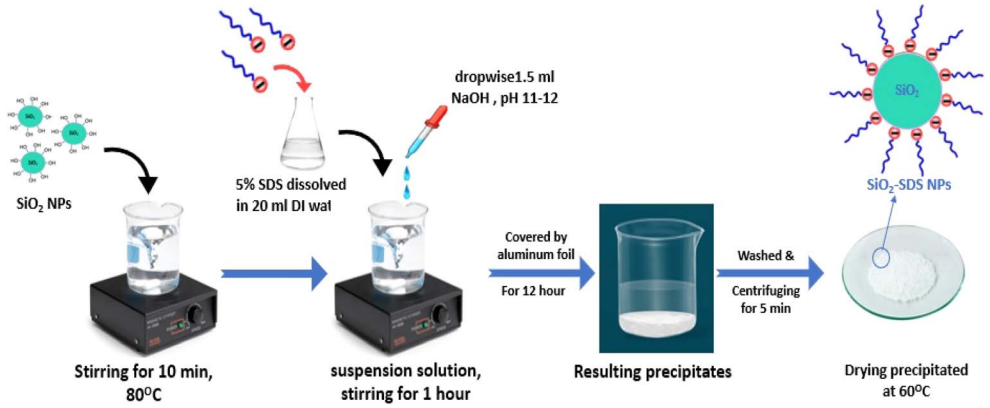

Fig. 1 Modifying SiO_2 NPs with SDS.

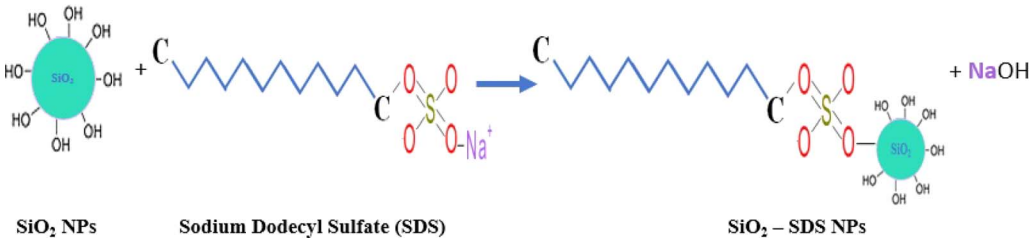

Scheme 1 The reaction process for the modified material SiO_2-SDS.

11 and 12. Furthermore, the solution was covered with aluminum foil and left overnight. The resulting precipitates were washed several times with de-ionized water to remove impurities and then centrifuged for 5 min to remove excess surfactant and water content. The final product was dried at 60 °C in an electrical oven under an air atmosphere. After heat treatment, coated silica nanoparticles SiO_2-SDS were formed (Fig. 1). The reaction process for the modified material SiO_2-SDS is shown in Scheme 1.

2.3. Mixed matrix membrane preparation

The polymer material (PVC) was dried in an oven at 60 °C for 4 h to remove moisture. The casting solution was prepared by adding dried 14 wt% PVC to 86 wt% DMAc solvent and then mixed overnight at 200 rpm and 40 °C to achieve a homogeneous dispersion. When a clear yellowish casting solution was obtained, SiO_2-SDS NPs were added with various weight percentages (*i.e.*, 0, 0.05, 0.1, 0.15, 0.2, and 0.25 wt%), and the solution was kept for 15 min in an ultrasonic bath to avoid nanoparticle aggregation. Table 1 shows the composition of the PVC/DMAc/SiO_2-SDS casting solution. It should be noted that the actual percentages are slightly different, but the values presented represent an acceptable approximation. The polymer solution was cast using an automatic film applicator (AFA-IV, China) of 200 μm thickness, as shown in Fig. 2, and was then placed in a coagulation bath for a minute, where the membrane detached from the glass plate, indicating completion of phase inversion.[39] Three sheets of the same membranes were selected for characterization and testing. The proposed synthesis process to prepare PVC/DMAc/SiO_2-SDS-based MMMs is considered to be a relatively sustainable approach compared to the synthesis of other membranes, such as fluoropolymers. In this process, PVC was used as the main component. This polymer has a lower environmental impact than fluoropolymers, whose synthesis is associated with emissions causing serious environmental issues, such as global warming, ecotoxicity, and ozone depletion.[40] Although the solvent used is not green, Hansen solubility calculations based on the parameters reported in ref. 41,42 indicate that PVC is incompatible with all available green solvents, leaving us no choice but to use a conventional solvent. The other components of the composite-silica NPs and SDS have a minimal environmental footprint compared to more complex chemicals and nanoparticles used in similar studies. It is noteworthy that this simple analogy cannot accurately evaluate the sustainability of the process, and more sophisticated tools should be employed,

Table 1 Composition of the prepared MMMs

Membrane code	PVC wt%	DMAc wt%	SiO_2-SDS wt%
PSS-0	14	86	0
PSS-0.05	14	86	0.05
PSS-0.1	14	86	0.1
PSS-0.15	14	86	0.15
PSS-0.2	14	86	0.2
PSS-0.25	14	86	0.25

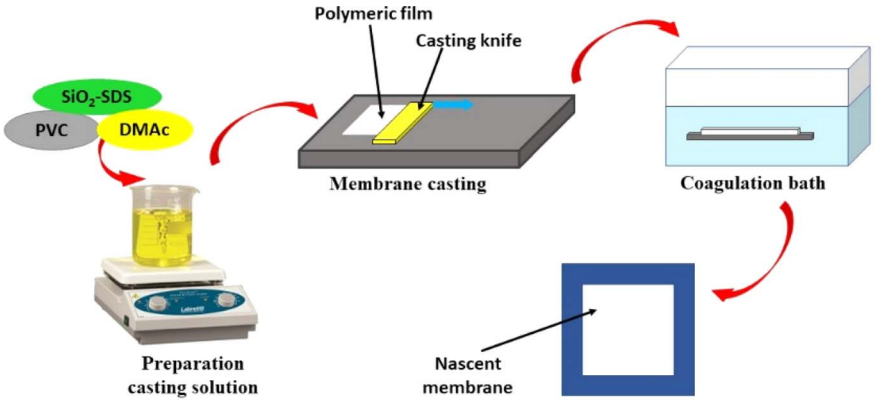

Fig. 2 Preparation of mixed matrix membranes.

such as life cycle assessment, which can explored as a future direction for this study.

2.4. Characterization of nanoadditives and mixed matrix membranes (MMMs)

Fourier transform infrared spectroscopy (FTIR) (model: ALPHA IR Fourier Spectrometer, Bruker) was utilized to study the structural changes in virgin membranes and MMMs. The measurements were taken for the wavenumber range 500–4000 cm^{-1}. The phase patterns of the samples were obtained using X-ray diffraction (XRD) (model XRD-6000 Shimadzu Tokyo, Japan). All samples were scanned using Cu Kα radiation with a wavelength $\lambda = 0.1542$ nm, at 2θ within the range of 10–90°, at 13 °C, at a speed of 10 ° min^{-1}.

The surface topography (2D and 3D images), and roughness of the MMMs were characterized using an atomic force microscopy (AFM) instrument with a Nova SPB scanning probe microscope (Ntegra Prima, Russia). The membrane surfaces were scanned with an image size $\geq$ (10 000 nm × 10 000 nm) and 512 topographic pixels. The morphology of the synthesized membrane was obtained by utilizing an SEM Tescan Vega (4 LMS instrument, Czech Republic). Scanning electron microscopy (SEM) (model: TESCAN Vega 4 LMS instrument, Czech Republic) was employed to observe the membrane surface and cross-sectional morphology. For membrane cross-section imaging, the samples were prepared by cutting the membranes in liquid nitrogen. To determine the thickness of the membranes, a thickness gauge (NOVOTEST TP-1) was used, and measurements were taken at various points of the membrane and then the average value of the measurements was reported.

The porosity of the membrane (ε%) was calculated as the pore volume divided by the overall volume of the membrane. The porosity was determined by cutting dry samples to a specific shape and weight. The membrane was then soaked in DI water overnight and the surface was wiped with filter paper to get rid of any excess water drops and weighed again. Eqn (1) was applied to calculate porosity:[43]

$$\varepsilon = 1 - \frac{\rho_m}{\rho_p} \quad (1)$$

where, ε% is the porosity; ρ_p is the polymer density (1.38 g cm^{-3}); and ρ_m is the membrane density (g cm^{-3}), which is found from eqn (2):

$$\rho_m = \frac{M}{L \times W \times I} \quad (2)$$

where M is the mass of the synthesized membrane (g); L, W, and I are the length, width, and thickness of the synthesized membrane, respectively, each measured in cm.

The mean pore radius (r_m) was determined using the Guerout–Elford–Ferry equation based on the results of the pure water flux and porosity calculations, as shown in eqn (3):[44]

$$r_m = \sqrt{\frac{(2.9 - 1.75\varepsilon)8\eta IQ}{\varepsilon A \Delta P}} \quad (3)$$

where r_m is the mean pore radius of the membrane (m), η is water viscosity (8.9 × 10^{-4} Pa s), I is the membrane thickness (m), Q is the permeate flow (m^3 s^{-1}), and ΔP is the operating pressure (Pa).

2.5. Performance evaluation

The carwash wastewater was obtained from one of the semi-automatic carwash stations in Yekaterinburg (Sverdlovsk region) from a sedimentation tank which is designed for the collection and preliminary treatment (settling) of wastewater. The chemical oxygen demand (COD) and total suspended solids (TSS) of the carwash wastewater were 220 mg O_2 per L and 649 mg L^{-1}, respectively. Before starting the work, simple pretreatment was carried out through sedimentation (24 h) and filtration (1-micron polypropylene filter) of the sample to meet the feeding requirements of the UF membrane.

Experiments on the permeability, wastewater rejection, and anti-fouling properties of the UF membranes were carried out using a laboratory-scale cross-flow filtration cell at a trans-membrane pressure of 1 bar and a temperature of 25 °C, as shown in Fig. 3a. The carwash wastewater was placed in the feed tank and circulated through the membrane module by a pump. The flat-sheet membrane module was designed with an outer area of about 54.76 cm^2 (5.8 cm × 8.7 cm), and an effective area of about 13.75 cm^2 (2.5 cm × 5.5 cm), as shown in Fig. 3b.

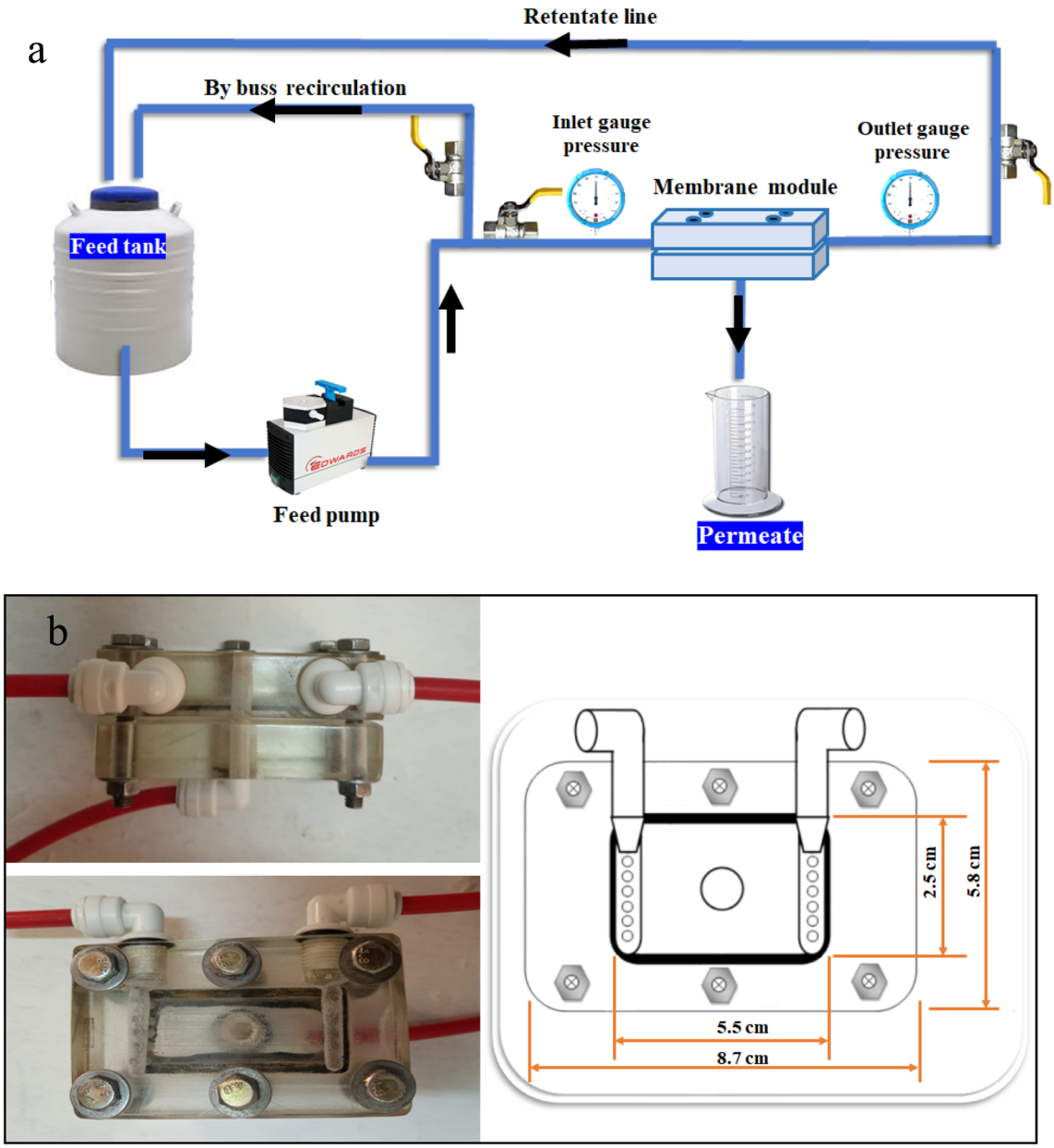

Fig. 3 (a) Schematic diagram of the cross-flow filtration unit. (b) Flat-sheet membrane module.

The pure water flux (L m^{-2} h^{-1}) was determined using the following equation:[45]

$$J = \frac{V}{A \times t} \quad (4)$$

where J is the flux (L m^{-2} h^{-1}), V is the permeate volume (L), A is the effective surface area of the membrane (m^2), and t is the time (h).

The membrane rejection (R%) of two important quality indicators, namely chemical oxygen demand (COD) and total suspended solids (TSS), were calculated with the following equation:[46]

$$R\% = \left[1 - \frac{C_p}{C_f}\right] \times 100 \quad (5)$$

where C_f and C_p are the concentrations of pollutants in the permeation and feed wastewater solutions, respectively.

Standard methods of analysis were used to determine the concentration of pollutants in wastewater and permeate.[47] The chemical oxygen demand (COD) was determined using the 5220 B method, which involves the action of a strong oxidizer (potassium bichromate in sulfuric acid) on organic impurities of wastewater under boiling conditions. Suspended solids (TSS) in carwash wastewater can be either organic or inorganic in nature, mainly consisting of sand and dust accumulating in car tires and on car surfaces, as well as some chemicals and detergents, and they were analyzed using the procedures described in method 2540 D.

To determine the flux recovery ratio (FRR) of the membranes, the pure water flux was first measured as J_{w1} for 90 min. It was then replaced by a carwash wastewater sample and operated for the same duration. After that, the fouled membranes were backwashed with DI water for 120 min, and the recovered flux of the cleaned membrane was calculated again as J_{w2} for 90 min. The flux recovery ratio (FRR) was calculated with eqn (6):[48]

$$\mathrm{FRR} = \frac{J_{w2}}{J_{w1}} \times 100\% \quad (6)$$

2.6. Statistical analyses

All the measurements were recorded at least twice, and the average values were reported. The statistical significance of the measured changes in the membrane characteristics and performance indicators was tested at a confidence interval of 95%. A *T*-test for one group was carried out and *t*-statistics and *p*-value were computed.

3. Results and discussion

3.1. Membrane characterization

3.1.1. FTIR test and XRD. FTIR analysis of pristine and modified membranes with SiO_2-SDS NPs are presented in Fig. 4. The FTIR spectrum of PSS-0 exhibits several bands characteristic of C–Cl, C–H, C=C and O–H groups. As observed from Fig. 4, the characteristic bands of pristine PVC can be classified into three regions. The first is the C–Cl stretching region in the range 800–600 cm^{-1}. The second region is C–C stretching in the range 1200–900 cm^{-1}. The third region is C=C stretching in the range 1425–1250 cm^{-1}.[49]

Following modification with SiO_2-SDS NPs, the asymmetrical and symmetrical Si–O–Si stretching appeared at 1026 and 511 cm^{-1}, respectively.[50] Therefore, peaks at approximately 1026 cm^{-1} confirmed the existence of Si–O–Si on the surface of the modified membranes, indicating that the SiO_2-SDS NPs had been successfully incorporated. It can be noticed that the intensity of the Si–O–Si peaks was enhanced progressively with an increase in the added concentration of SiO_2-SDS NPs, indicating that more SiO_2 NPs had accumulated in the membrane surface.[51]

The peak at 2927 cm^{-1} corresponds to the stretching vibration absorption of –OH groups. Remarkably, the intensity of this peak increased with an increase in the amount of SiO_2-SDS NPs added, indicating that the addition of more SiO_2-SDS NPs led to an increase in the amount of –OH groups on the surface of the modified membranes, which has a positive impact on improving their performance.[52]

X-ray diffraction (XRD) is a powerful technique to identify crystalline phases in materials. An amorphous phase is typically observed in PVC.[53] Full-range measurement for MMMs can be used to examine the effect of inorganic NPs. Fig. 5 shows the X-ray diffraction of pristine PVC and MMMs. Examination of the XRD diffraction patterns of a pristine PVC membrane and PVC containing 0.05 wt% of SiO_2-SDS NPs reveals no discernible peak, indicating that this small percentage of additive was not enough to cause a significant change in the amorphous nature of PVC. However, a further increase in the SiO_2-SDS NP content beyond 0.05 wt% leads to the appearance of two sharp intense peaks at about $2\theta = 13°$ (220) and 16° (311), attributed to the

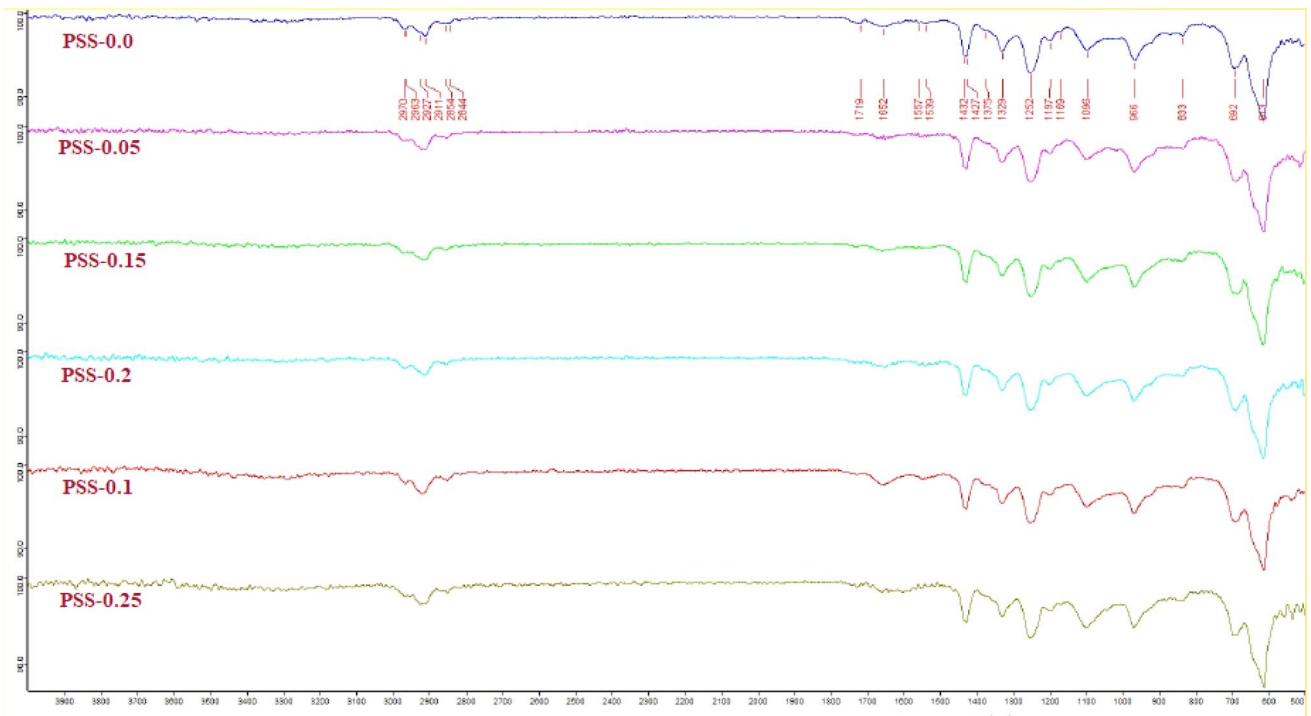

Fig. 4 FTIR of the pristine membrane and MMMs.

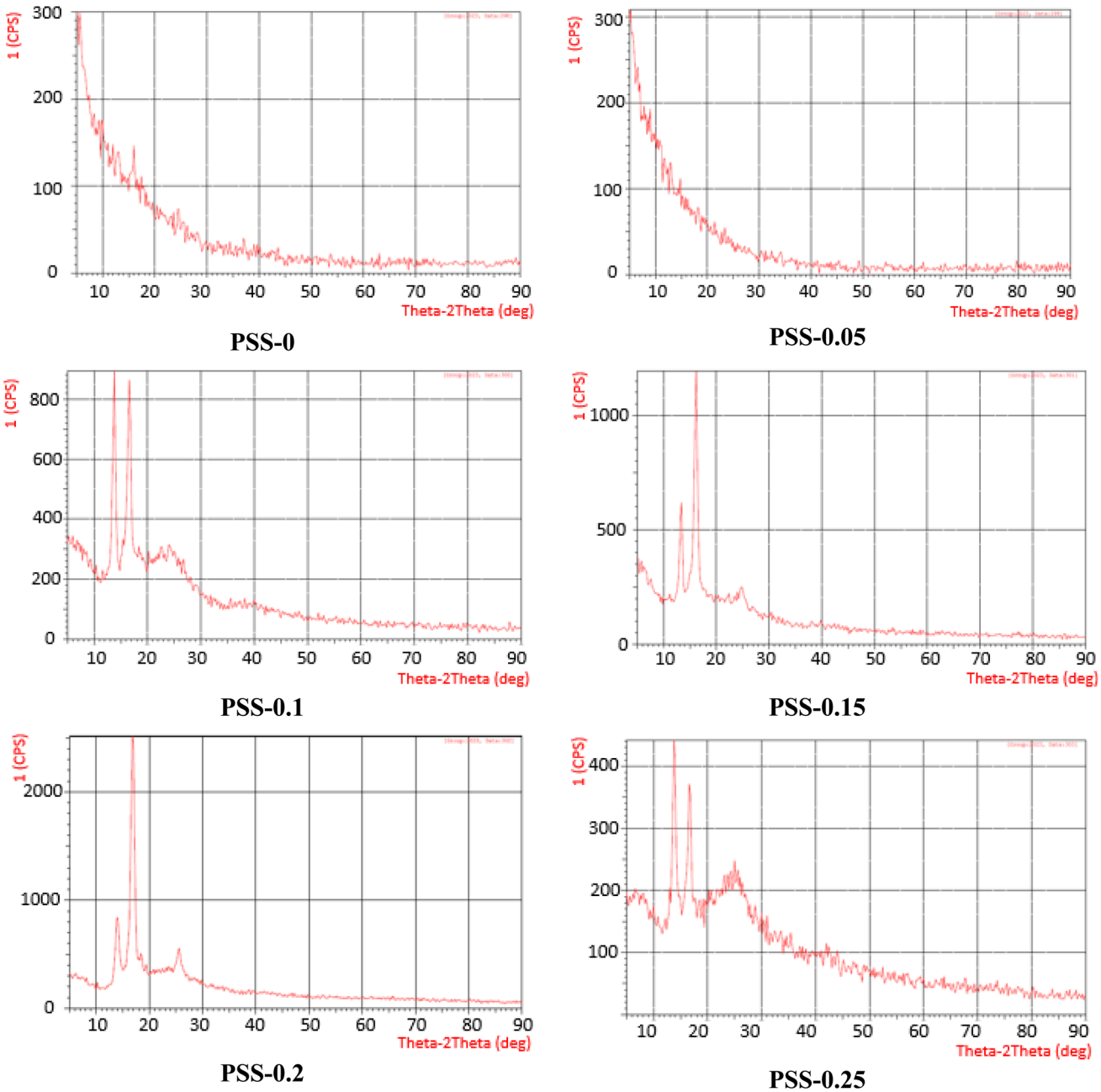

Fig. 5 XRD of the pristine membrane and MMMs.

presence of separated crystalline phases within the polymeric matrix (JCPDS card no. 19-0629). A small peak with low intensity appeared at 24° (422), indicating the successful incorporation of SiO_2-SDS NPs into the membrane surface.[54] Additionally, it was noted that the amorphous halos of MMMs were less intense than those found in the pristine PVC membrane pattern. This suggests that the addition of NPs alters the amorphous nature of PVC membranes and points to the formation of multiple phases in the MMMs that are made up of a combination of semicrystalline and amorphous phases.[55]

3.1.2. Atomic force microscopy (AFM) analysis. Fig. 6 and 7 show the two and three-dimensional surface AFM images of the top surfaces of the PVC membranes prepared with several different amounts of SiO_2-SDS NPs in the PVC casting solution. In these 2D and 3D images, the brightest regions represent the highest area of the material surface and the dark regions indicate the lowest areas of the membrane.[56]

For the AFM analysis, the roughness parameters were calculated for a scanned area of 10 nm × 10 nm. Surface roughness is considered the most important factor for improving the antifouling ability of membranes.[57] The surface roughness parameters of the membranes, which are determined in terms of the average roughness (Ra), the root mean square (Rq), and the mean difference between the highest peaks

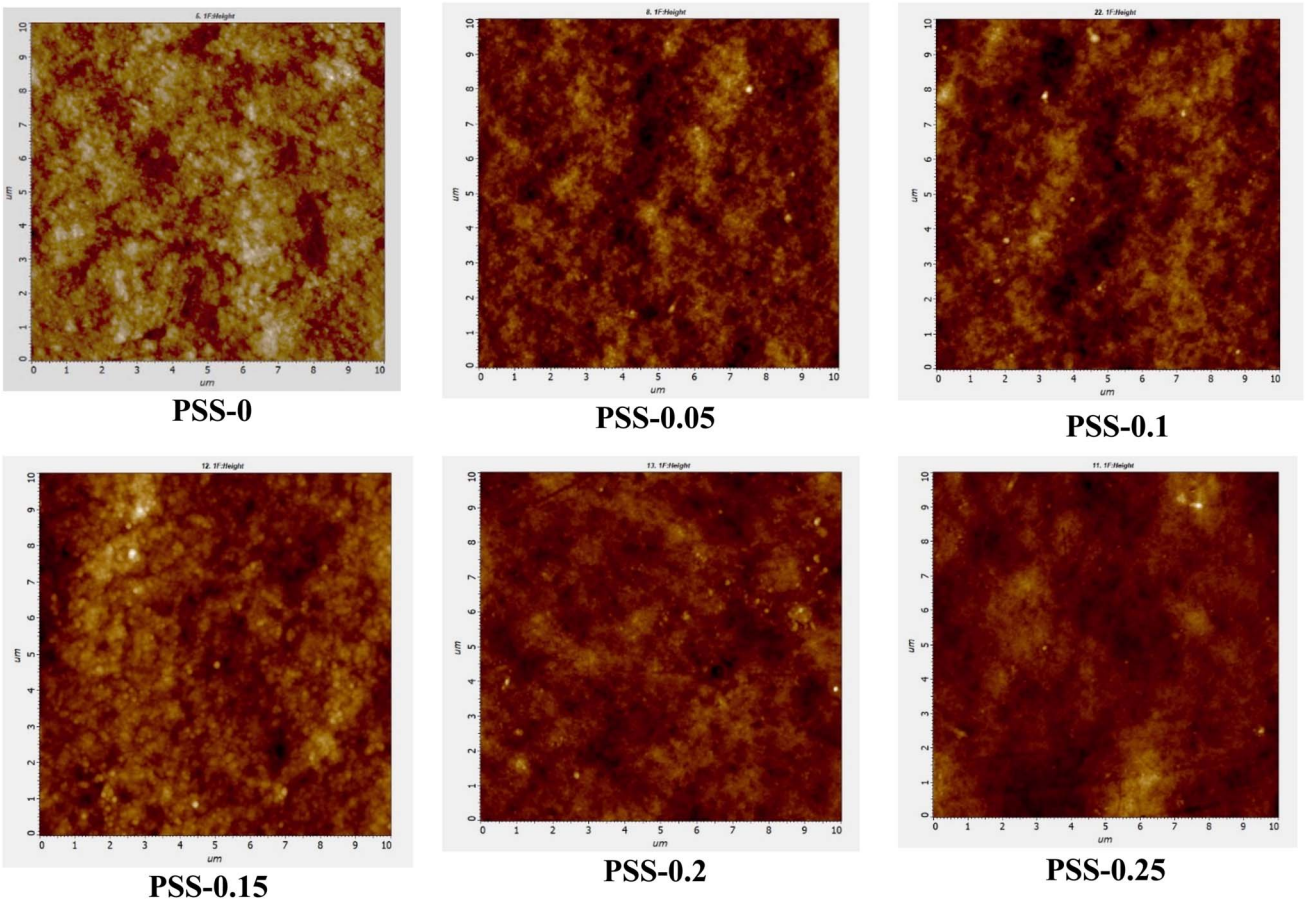

Fig. 6 2D AFM images of the top surface of the pristine membrane and MMMs.

and lowest valleys (Rz), are shown in Table 2. The Ra, Rq, and Rz values of the modified membranes were significantly different from those of the pristine membrane, with corresponding *p*-values of 0.0180, 0.0200, and 0.0065.

The 2D and 3D surfaces exhibited small and densely distributed nodules for the pure PVC membrane (PSS-0), as depicted in Fig. 6 and 7. The addition of 0.05, 0.1, and 0.15 wt% of SiO_2-SPS to the PVC casting solution resulted in an increase in nodule size and a decrease in their density on the surfaces of PSS-0.05, PSS-0.1, and PSS-0.15. The effect on the surface characteristics of the modified membranes following the addition of nanoadditives is in agreement with earlier research.[35] This merging of nodules can increase the membrane selectivity, owing to the availability of water absorption sites, indicating effective performance.[58]

The membrane surface seems to be rougher after adding SiO_2-SDS nanoparticles. As can be seen in Table 2, a growing trend in the roughness of the membrane surface could be observed by increasing the content of SiO_2-SDS nanoparticles. When 0.15 wt% of SiO_2-SDS NPs were added, the Ra value increased from 5.597 nm for the pristine membrane (PSS-0) to 8.364 nm for PSS-0.15, the Rq value increased from 7.080 nm (PSS-0) to 10.403 nm (PSS-0.15), and the Rz value increased from 59.050 nm to 100.325 nm. The increase in membrane roughness might be attributed to the incorporation of nanoparticles on the membrane surface. A membrane with a rougher surface has a greater tendency towards the deposition of particles on its surface. The particles accumulate in the valleys of the rough membrane surface. Subsequently, fouling becomes more severe for membranes with a rougher surface.[59] However, simultaneously, the increase in roughness may increase the hydrophobicity of the membrane surface,[60] leading to weaker interaction between foulants and the membrane surface. Whereas the addition of more NPs led to a slight decrease in mean roughness to 6.143 nm for PSS-0.2, but it is also rougher than the pristine membrane (PSS-0). This is mainly due to the accumulation of more NPs on the surface of the membranes, as shown in Fig. 5 and 6. The mean pore size of a membrane can affect its roughness. Different studies have shown that membranes with larger pore sizes tend to have higher roughness values than membranes with smaller pore sizes.[61]

3.1.3. Scanning electron microscopy (SEM) analysis. The top-surface SEM images of the pristine membrane and MMMs are presented in Fig. 8. As shown in this figure, the surface morphology of PSS-0.0 presented a rough surface with some pores dispersed on the surface due to the higher amount of PVC at the film interface, which results in fewer pores on the top layer of the membrane.[62,63] After modification, the surface became more porous due to the presence of SiO_2-SDS NPs in the surface of the PSS-0.05, PSS-0.1, and PSS-0.15 membranes.

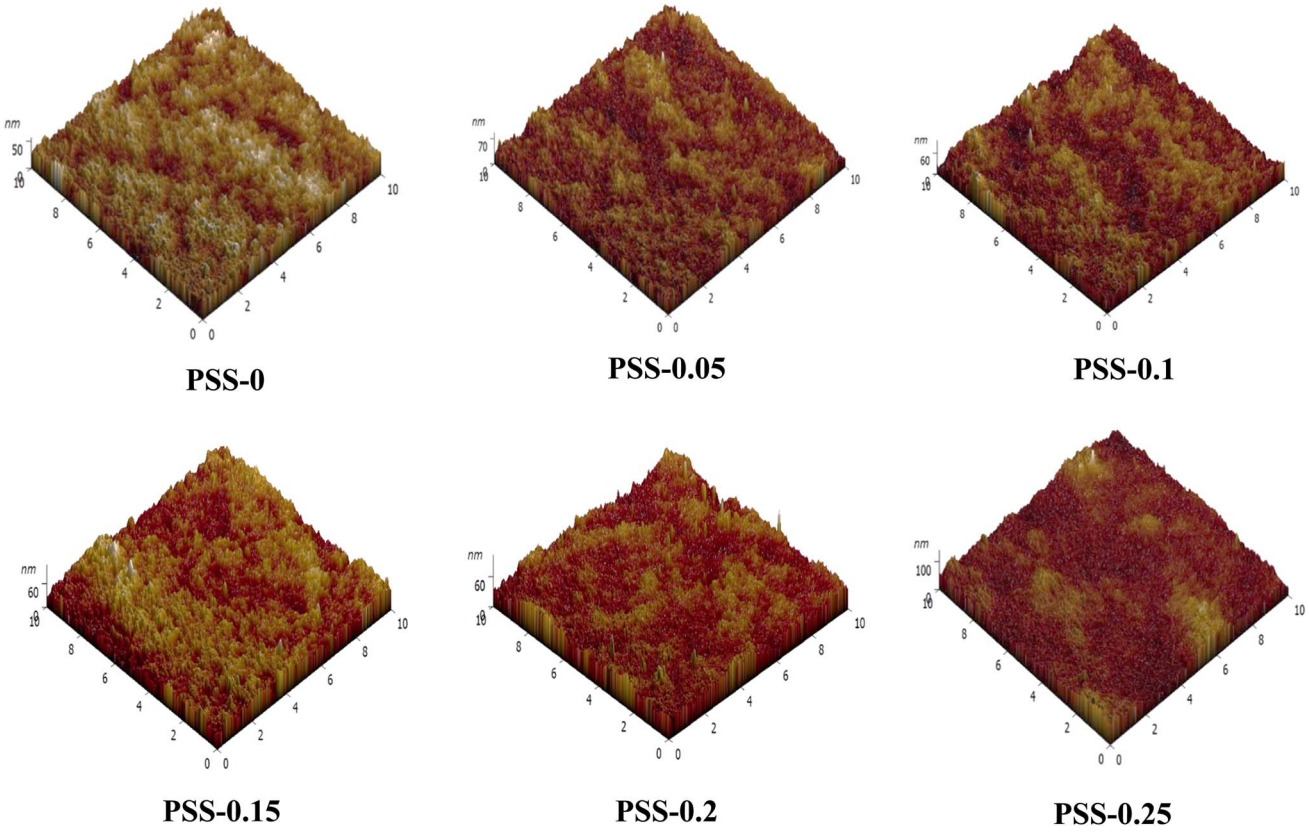

Fig. 7 3D AFM images of the top surface of the pristine membrane and MMMs.

Table 2 The surface roughness parameters from the AFM images[a]

Membranes	Average roughness (Ra), nm	Root mean square (Rq), nm	Distance between the highest peak and lowest valley (Rz), nm
PSS-0	5.597	7.080	59.050
PSS-0.05	7.023	8.873	89.939
PSS-0.10	8.248	10.403	100.325
PSS-0.15	8.364	10.662	109.499
PSS-0.20	6.143	7.833	102.962
PSS-0.25	9.580	12.455	146.930

[a] PVC/SiO_2-SDS is denoted as PSS.

However, an important increase in the amount of SiO_2-SDS NPs may block the layers due to the accumulation of SiO_2 NPs on the surface of PSS-0.2 and PSS-0.25 membranes.[30,64]

Fig. 9 shows the SEM images of the cross-sectional structures of the pristine and modified membranes with SiO_2-SDS NPs. The images confirm that the addition of SiO_2-SDS NPs up to 0.15 wt% did not affect the morphology and the asymmetric structures of the membrane cross-sections. The SEM images revealed that a thin filtration layer on the top surface of the membrane appeared with a supporting layer with macro-voids at the bottom. The top layers of the membranes significantly increased with an increase in the amount of SiO_2-SDS NPs added. However, the cross-sectional structure of the PSS-0.2 and PSS-0.25 membranes seems to be affected by the addition of large amounts of SiO_2-SDS NPs. The deformation of the cross-sectional structure of the PSS-0.2 and PSS-0.25 membranes may be due to the accumulation of NPs in their cross-sectional structure, which block the layer.[65]

3.1.4. Thickness, porosity, and mean pore size. Fig. 10 shows the effect of SiO_2-SDS NPs on the thickness and porosity of a pristine membrane and MMMs. With an increase in the SiO_2-SDS NP concentration up to 0.15 wt%, the membrane thickness and porosity increased.

The highest thickness was 118.71 ± 0.42 μm for PSS-0.15 MMMs. The thickness of PSS-0 was 100.21 ± 0.76 μm, which increased to 109.05 ± 0.64 μm and 113.35 ± 0.64 μm when the concentrations of SiO_2-SDS NPs in the casting solution were 0.05 and 0.1 wt%, respectively. These differences in the

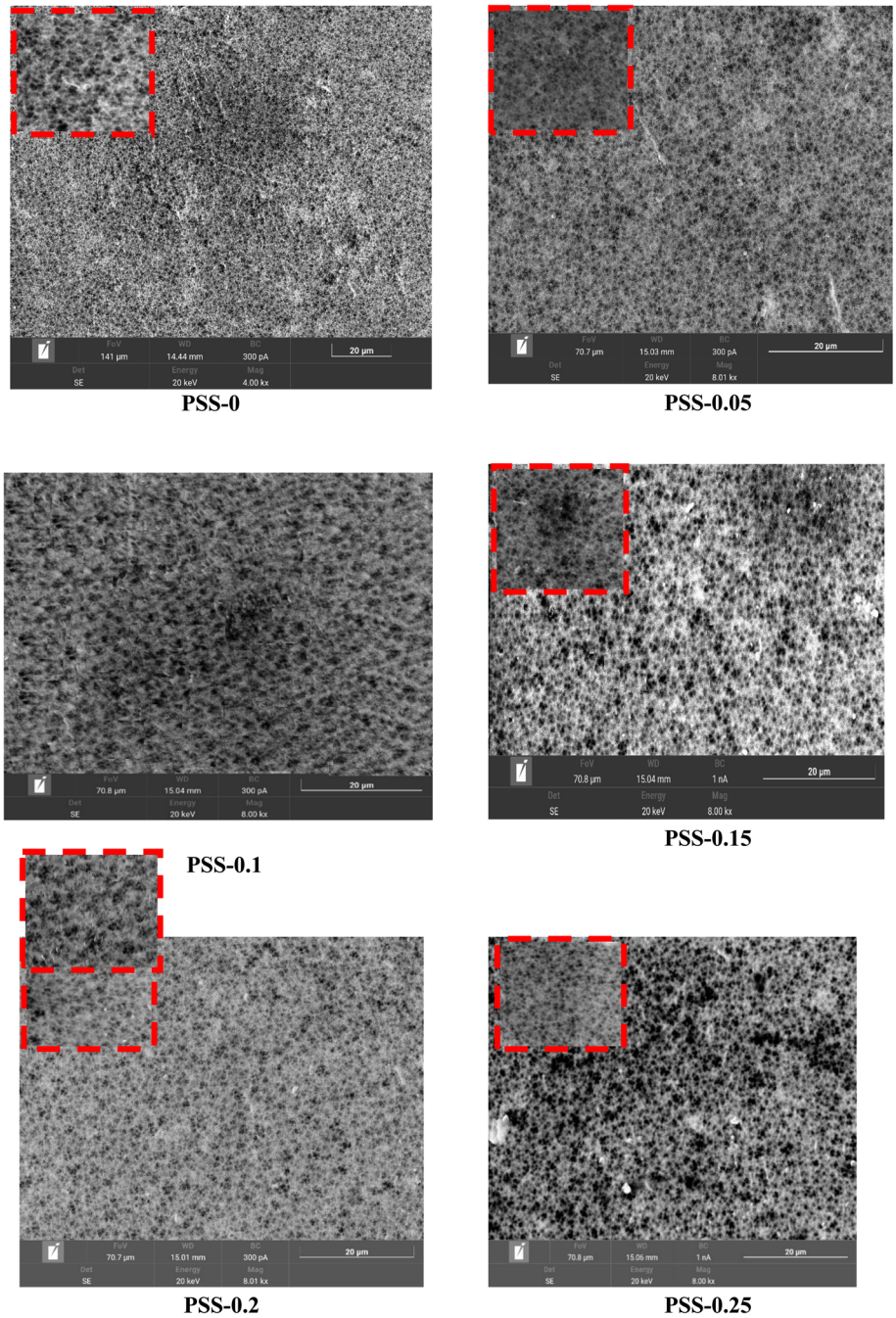

Fig. 8 SEM of the top surface of the pristine membrane and MMMs.

membrane thickness are statistically significant with a *p*-value of 0.0270. These results were likely due to the increase in the viscosity of the doping solution upon the addition of nanoparticles.[66]

The measured porosity of the pristine membrane (PSS-0) was 78.62 ± 1.21%. Increasing the content of nano-additives increased the porosity to around 80.19 ± 0.77% for the PSS-0.05 MMMs. This increase continued to a maximum porosity of 81.40 ± 0.23% for the PSS-0.15 membrane. The calculated *p*-value for the increase in porosity was found to be 0.0002, confirming that the increase is statistically significant. Similar results were reported in ref. 67. Adding 0.2 wt% SiO_2-SDS NPs decreased the porosity to 80.07 ± 0.81%. This drop could be due to the increase in viscosity of the doping solution, which may function as a source of resistance, resulting in a delayed liquid–liquid demixing process.[68]

The mean pore size is a very important factor affecting the permeate flux of a UF membrane. The mean pore diameters of the pristine membrane and MMMs are shown in Fig. 11. It can be seen from the figure that as the amount of SiO_2-SDS NPs increased, the mean pore diameter increased from 30 nm for the pristine membrane (PSS-0) to 39 nm for PSS-0.05 until it

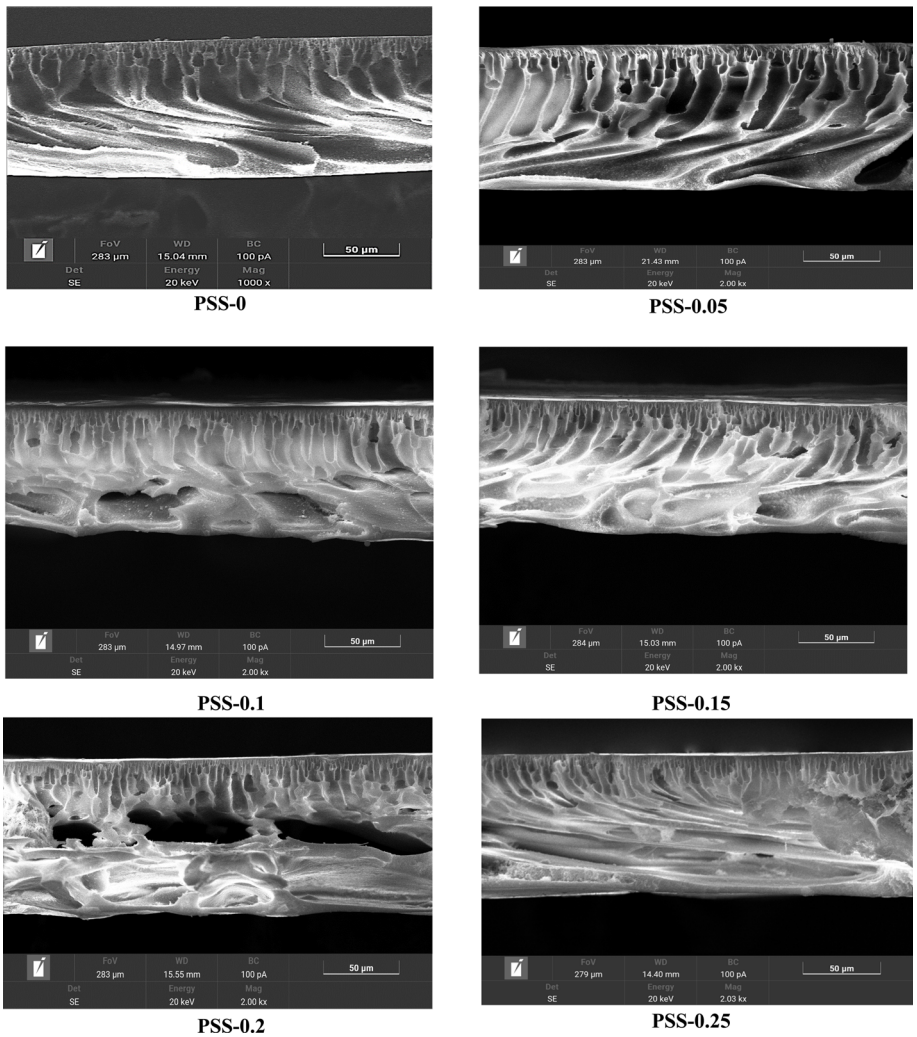

Fig. 9 SEM of the cross-sectional structure of the pristine membrane and MMMs.

reached a maximum of 45 nm for PSS-0.15. From a statistical standpoint, the pore diameter of modified membranes was found to be significantly different from that of the pristine membrane (p-value = 0.0092). This increase could be a result of the enhanced exchange rate between the solvent and non-solvent during membrane formation induced by the addition of SiO_2-SDS NPs to the casting solution.[62,66] A further increase in SiO_2-SDS NPs resulted in a drop in pore size, probably due to NP accumulation on the membrane surface.

3.2. MMM performance evaluation

3.2.1. Pure water flux. Fig. 12 shows the effect of different concentrations of SiO_2-SDS NPs on the pure water flux at room temperature and a pressure of one bar. Generally, all the modified membranes had a higher pure water flux. The results show that by adding 0.05 wt% SiO_2-SDS NPs (PSS-0.05), the pure water flux increased from 65.2 ± 2.4 L m^{-2} h^{-1} for PSS-0 to 104.97 ± 2.4 L m^{-2} h^{-1}. The pure water flux continued to show a significant increase after the addition of SiO_2-SDS NPs, reaching its highest value of 127.75 ± 1.72 L m^{-2} h^{-1} at 0.15 wt%. The increasing trend in pure water flux was consistent with the pore size, porosity, and membrane morphology and with the structure of the supporting layer with macro-voids in the modified membranes, as shown in earlier sections. However, the addition of 0.2 and 0.25 wt% of SiO_2-SDS NPs resulted in a reduction in pure water flux to about 101.09 ± 7.88 and 102.30 ± 6.17 L m^{-2} h^{-1}, respectively. This reduction could be attributed to pore blockage due to agglomeration of the high content of SiO_2-SDS NPs.[69]

3.2.2. TSS and COD rejection from carwash wastewater. The rejection of TSS and COD by the prepared membranes was calculated, and the results are presented in Fig. 13. UF membranes possess the capacity to effectively remove TSS and COD due to their size exclusion mechanism.[70,71] The removal of COD may also be explained by adsorption, where particles are captured inside the membrane structure, which permits the removal of particles smaller than the membrane pores.[72] As indicated in Fig. 13, TSS rejection by MMMs was improved in comparison to the pristine membrane. Although the pristine membrane has the smallest pore size, which should show the highest rejection, a possible explanation for this deviation is the

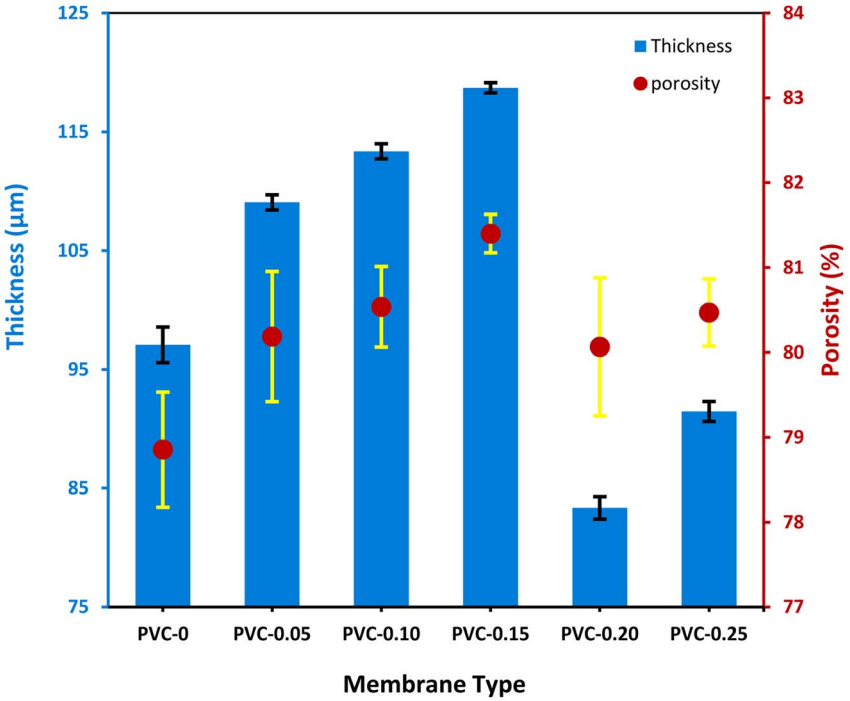

Fig. 10 PVC/SiO_2-SDS MMMs porosity and thickness compared with the pristine membrane.

contribution of surface roughness to hosting TSS and organic carbon, which could alter the pore size profile for the modified membrane, leading to a better rejection compared to the virgin membrane. Another factor that might have played a role is that the increase in porosity is accompanied by an increase in tortuosity and the longer path for small particles might lead to their entrapment and consequent increased rejection.[73]

The incorporation of rejection by SiO_2-SDS NPs into PVC led to a significant improvement in the removal of both model contaminants, COD and TSS, gauged by the calculated *p*-values

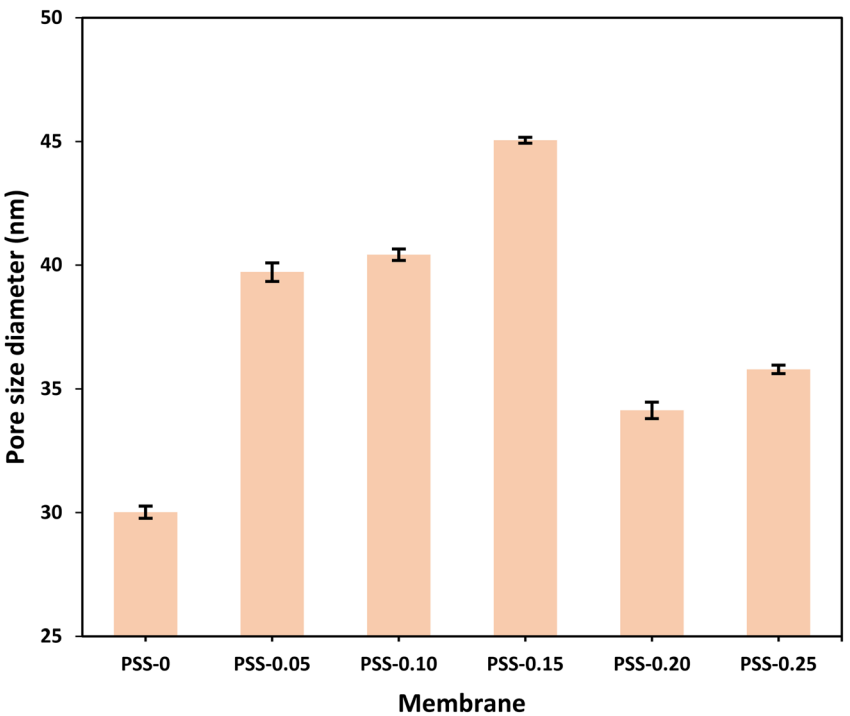

Fig. 11 PVC/SiO_2-SDS MMMs mean pore size diameter compared with the pristine membrane.

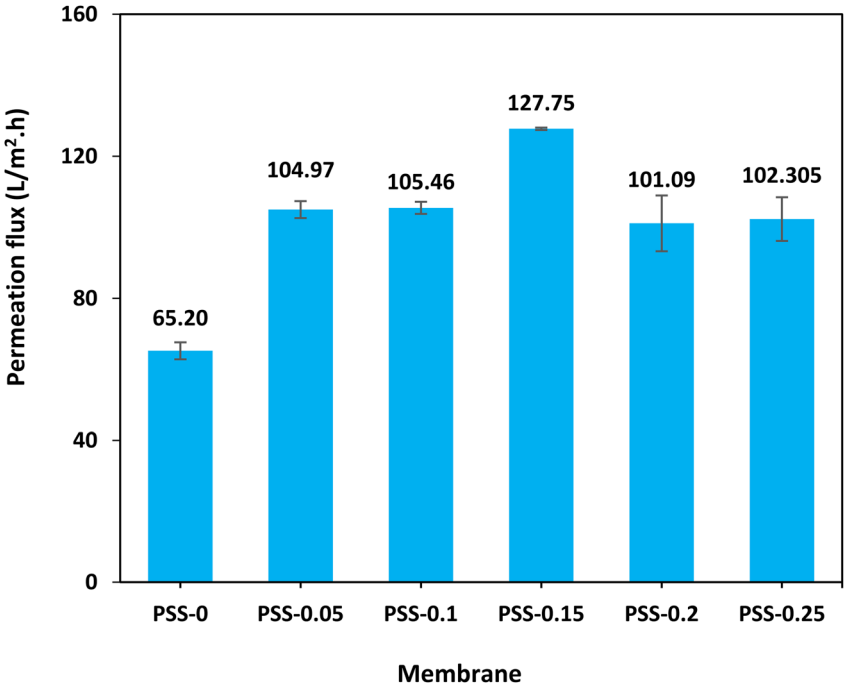

Fig. 12 Pure water flux of a pristine membrane and MMMs prepared with different concentrations of SiO_2-SDS NPs. The increase in permeate flux of the modified membranes is statistically significant compared to that of the pristine membrane (p-value = 0.0009).

of 0.0018 and 0.0065, respectively. PSS-0.05 and PSS-0.1 show close TSS rejection rates of 94.25 ± 1.04% and 95.81 ± 1.69%, respectively. The rejection value declined by about 1–2.3% for PSS-0.15 in comparison with PSS-0.05 and PSS-0.1, due to the membrane surface having a higher percentage of large pores which agrees with AFM results. Additionally, the PSS-0.1 membrane demonstrated the highest COD rejection of 81.18 ± 1.09%. It was observed that the pristine membrane had a COD rejection of approximately 64.85 ± 1.16%, while all the MMMs prepared with different concentrations of SiO_2-SDS NPs exhibited a COD rejection rate of over 72%. The ultrafiltration system effectively eliminated suspended solids, as evidenced by the TSS test results. Organic matter in the wastewater existed in soluble form, as colloidal particles, or adhered to the outer

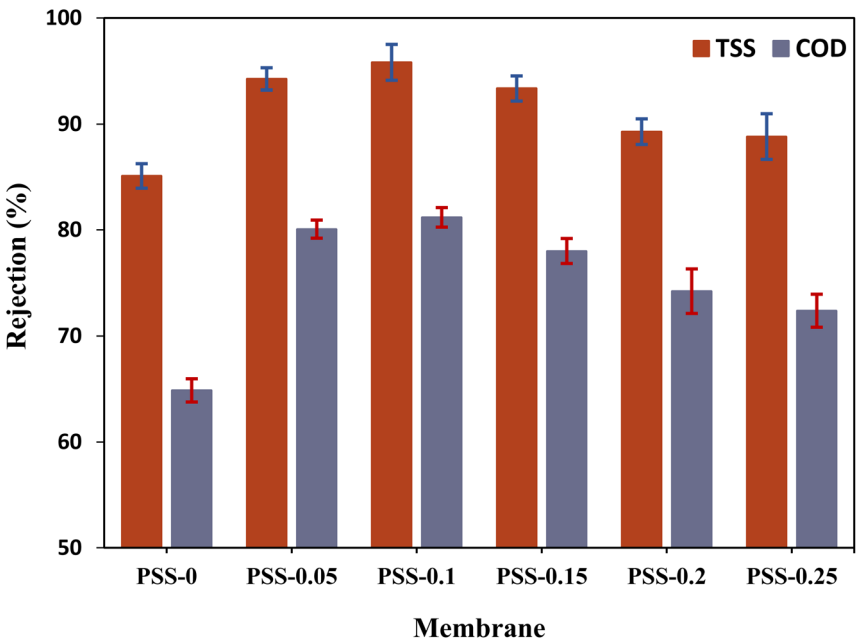

Fig. 13 Rejection% for total suspended solid (TSS) and COD for carwash wastewater by the pristine membrane and MMMs (25 ± 1 °C, and 1 bar).

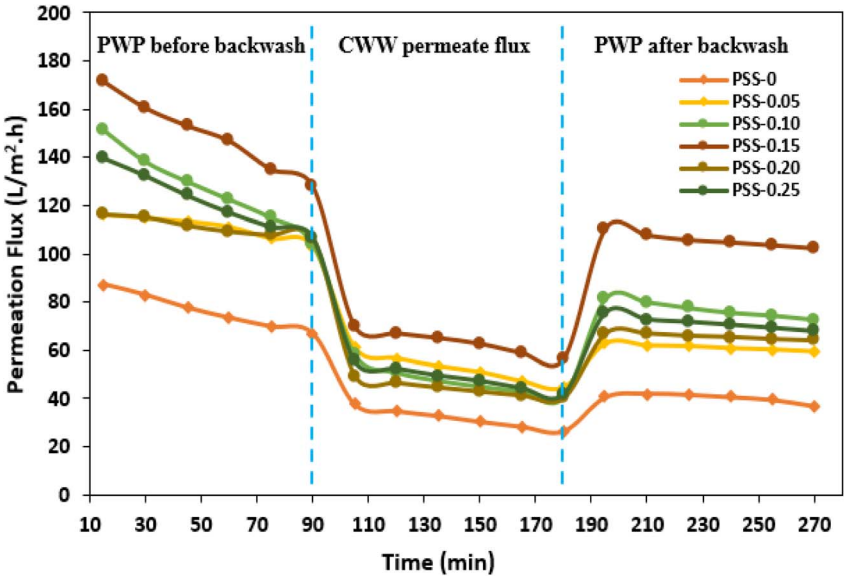

Fig. 14 Time-dependent permeation flux for the pristine membrane and MMMs, as follows: the first 90 min for pure water flux, the second 90 min for flux of carwash wastewater (CWW) and the third for pure water flux after the fouled membranes had undergone one hour of back-flushing with pure water.

surface of the suspended solids. By removing the suspended solids, the organic matter was partially eliminated, which contributed to the improvement in COD rejection. In contrast, the ultrafiltration membrane retained some organic material larger than its pore size, resulting in a reduction in organic material in the permeate.[74]

3.2.3. Flux recovery ratio. After the membranes are used with wastewater, they need to be able to regain their water flux, which is crucial for their effectiveness. If the membranes cannot regain their water flux, this can lead to reduced filtration performance and a lower quality of treated water.[75] Therefore, it

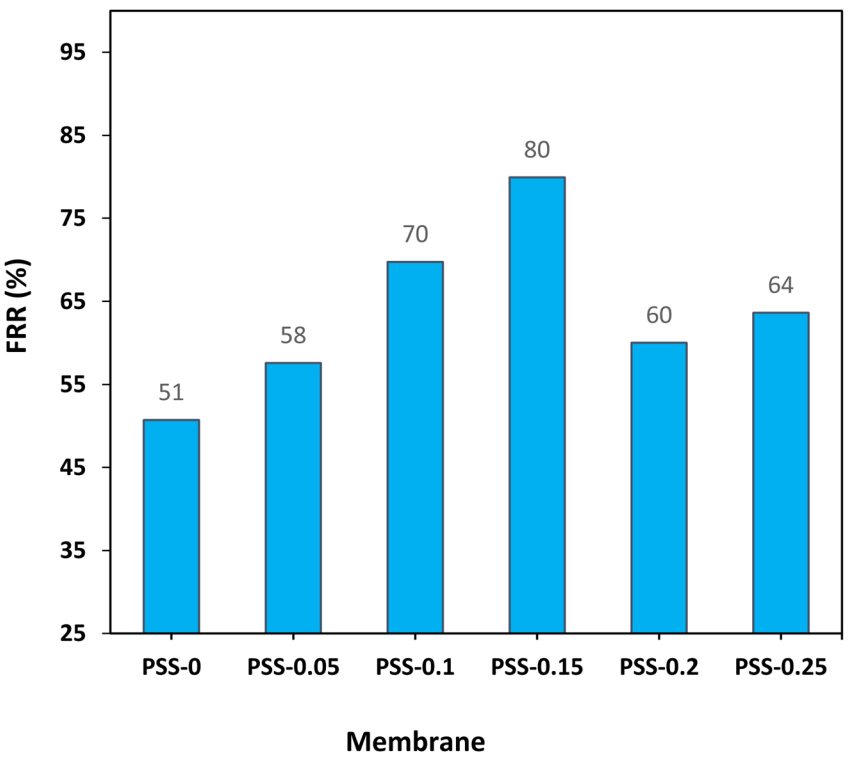

Fig. 15 The flux recovery ratio (FRR) of the pristine membrane and MMMs. The observed changes in the MMMs were found to be statistically significant with a p-value of 0.0178.

is imperative to assess and compare the water flux of membranes before and after fouling to ensure their functionality and reliability. Following the ultrafiltration test, the membranes were cleaned, and the pure water fluxes were measured once more, as shown in Fig. 14. After backwashing, the pure water flux was lower than before backwashing and the membranes were unable to recover their water flux as a result of irreversible fouling. This decrease in pure water flux can be attributed to contaminants trapped in membrane pores or strongly adhered to the surface of the membrane even after backwashing.[76] Fig. 14 shows that the PSS-0.15 membrane showed the highest capacity for flux restoration compared to PSS-0 and other membranes, which suffer severe irreversible fouling.

Membrane fouling resistance is typically studied by analyzing the flux recovery ratio (FRR). Increased values of FRR signify enhanced membrane performance in terms of mitigating fouling effects during the operation of UF processes. Values of FRR for all MMMs were noticeably higher than those of the virgin PVC membrane (Fig. 15). The highest FRR observed was 80% for the PSS-0.15 membrane, in comparison to the unmodified membrane with an FRR of 51%. The low fouling tendency of the modified membranes could be due to the presence of large amounts of –OH groups in the modified membranes with SiO_2-SDS NPs that interacted with the Cl atoms of PVC chains through hydrogen bonds, forming a hydrophilic layer in the surface and within the structure of the membranes (Scheme 2), preventing the hydrophobic substance from adsorption or attachment onto the membranes. The increased connectivity between the membrane macro-voids could be another reason for the improved antifouling properties of the membranes.[37] The presence of SDS in the modified membranes can also enhance their antifouling by reducing surface tension and hindering the interaction between the membrane surface and foulants.[77]

Subsequently, the FRR decreased for the PSS-0.2 and PSS-0.25 membranes, which contained 0.2 and 0.25 wt% of SiO_2-SDS nanoparticles due to an increase in pore blockage.

Table 3 presents a performance comparison between the SiO_2-SDS polyvinyl chloride nanocomposite membranes prepared in the current work with those reported in the literature. The separation characteristics as well as the porosity of the

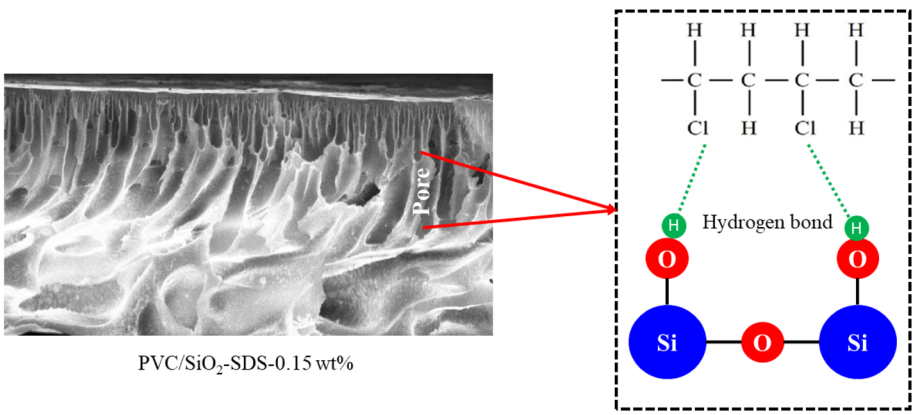

Scheme 2 Antifouling mechanism of the membranes modified by SiO_2-SDS NPs.

Table 3 Prepared membrane performance *versus* values reported in the literature

Membrane type	Porosity (%)	MWCO (kDa)	Wastewater type	Rejection (%)	Flux recovery ratio (%)	Reference
PES (GE osmonics)	—	10	Carwash	COD: 74	27	78
PAN/Ultrafilic (GE osmonics)		50	wastewater	COD: 73	39	
ABS/PEG/NMP	—	—	Carwash wastewater	COD: 70, TDS: 34, turbidity: 99	—	79
Polyamide/PSF-polyester	—	0.18	Oily wastewater	COD: 84	Long-term operation of 8 h with stable final flux	80
CA/SPEEK/Bentonite	37	—	Carwash	COD: 60, turbidity 88.6	85	81
PES/SPEEK/Bentonite	32	—	wastewater	COD: 47, turbidity 82	79	
PES/SiO_2/PEG	41	—	Oily wastewater	COD: 82, TDS: 47, NH_3: 67	—	82
PVDF/TiO_2	—	—	Reactive green 19 dye solution	COD: 63	—	83
PVC/SiO_2-SDS	81	—	Carwash wastewater	COD: 81, TSS: 93	80	This study

membranes are summarized in Table 3. It can be seen that the SiO_2-SDS polyvinyl chloride nanocomposite membranes show good COD rejection efficacy, and flux recovery ratio (%) in comparison with membranes reported in the literature. It can be seen that our membrane was superior in terms of COD rejection and flux recovery to other membranes, highlighting the high potential of the proposed composite for application to carwash wastewater treatment.

4. Conclusions

In the present study, the surface of SiO_2 NPs was modified with SDS and then they were used as an additive for PVC membranes to be used in carwash wastewater treatment. The successful incorporation of SiO_2-SDS NPs into PVC membranes, as indicated by SEM, EDX and FTIR analyses, improved their porosity and pore size and ultimately led to an improvement in their overall performance.

Based on the findings:

(1) The membranes prepared using SiO_2-SDS NPs exhibited considerable improvement compared to the virgin membranes, especially with the optimum content of SiO_2-SDS NPs of 0.15 wt%. This percentage resulted in the highest thickness of 118.71 ± 0.42 μm and maximum porosity of 81.40 ± 0.23%.

(2) The prepared membrane achieved the highest pure water flux of 127.75 ± 1.72 L m^{-2} h^{-1}, which is almost double that of the virgin membrane. When tested with carwash wastewater, PSS-0.15 produced higher TSS and COD rejection compared to the virgin membrane (93.35% *vs.* 85.10% and 78.01% *vs.* 64.86%, respectively). PSS-0.1 showed the highest rejection of TSS and COD among all tested membranes with 95.81% and 81.18%, respectively.

(3) The variation in TSS and COD rejection was likely due to the differences in porosity, roughness, and tortuosity that impact the interaction of colloids and organic materials with the membrane. Membrane efficiency restoration gauged by FRR showed that PSS-0.15 suffers the least irreversible fouling, highlighting its superiority among all the membranes and confirming that the percentage of SiO_2-SDS NPs was at its optimal level.

(4) It would be useful for future studies to test the performance of the prepared SiO_2-SDS/PVC MMMs for the removal of oil and grease and TDS from carwash wastewater, and pretreating domestic wastewater for water reclamation and reuse applications. However, some technical challenges need to be overcome to realize this in practice, including:

(i) Producing PVC-based membranes on a large scale encounters significant obstacles, such as fouling and poor mechanical properties. To enable the large-scale manufacturing of PVC-based membranes, it is crucial to enhance their environmental durability, and mechanical resilience, and to reduce their environmental impact.

(ii) Carwash wastewater often contains oil and grease that may cause several problems, such as constrained permeation performance, low stability, and a limited lifespan. Nonetheless, enhancing the permeance performance and resistance against such pollutants and fouling can be achieved through effective functionalization of the PVC surface chemistry. Techniques such as tuning the surface charge, incorporating functional materials on PVC surfaces, and utilizing nanoparticles to create pores could offer promising potential for mitigating the abovementioned issues and enhancing the practical application of the membranes. The results observed in this study suggest the same; however, testing the membrane for the removal of other contaminants, such as grease and TDS would be a valuable continuation of the current investigation in the future.

(iii) PVC-based membranes have exhibited promising antibacterial potential; however, there is a need for further research to fully uncover their capabilities and the mechanism of antimicrobial activity, taking into account their biocompatibility and cytotoxicity. In this context, machine learning and artificial intelligence approaches could advance membrane design and develop methods to predict the toxicity of experimentally generated PVC-based MMMs. These approaches would contribute to the safe-by-design optimization of PVC membranes for environmental applications.

Data availability

All data obtained in this study are presented in the manuscript.

Conflicts of interest

There are no conflicts to declare.

References

1 W. Musie and G. Gonfa, Fresh water resource, scarcity, water salinity challenges and possible remedies: A review, *Heliyon*, 2023, **9**(8), e18685. https://linkinghub.elsevier.com/retrieve/pii/S2405844023058930.

2 E. Shakir, Assessment of nutrient content of raw water close to water treatment plants located in Baghdad City, *Desalin. Water Treat.*, 2016, **57**(39), 18229–18233.

3 G. M. Jaid, A. A. AbdulRazak, H. Meskher, S. Al-Saadi and Q. F. Alsalhy, Metal-organic frameworks (MOFs), covalent organic frameworks (COFs), and hydrogen-bonded organic frameworks (HOFs) in mixed matrix membranes, *Mater. Today Sustain.*, 2024, **25**, 100672. https://linkinghub.elsevier.com/retrieve/pii/S2589234724000083.

4 E. S. Awad, S. M. Abdulla, T. M. Sabirova and Q. F. Alsalhy, Membrane techniques for removal of detergents and petroleum products from carwash effluents: a review, *Chim. Techno Acta*, 2023, **10**, 1–12.

5 S. Consoli, C. Caggia, N. Russo, C. L. Randazzo, A. Continella, G. Modica, *et al.*, Sustainable Use of Citrus Waste as Organic Amendment in Orange Orchards, *Sustainability*, 2023, **15**(3), 2482. https://www.mdpi.com/2071-1050/15/3/2482.

6 N. Alqadhi, M. H. Abdellah, S. Nematulloev, O. F. Mohammed, M. A. Abdulhamid and G. Szekely, Solution-processable poly(ether-ether-ketone) membranes for organic solvent nanofiltration: from dye separation to pharmaceutical purification, *Sep. Purif. Technol.*, 2024, **328**,

125072. https://linkinghub.elsevier.com/retrieve/pii/S1383586623019809.
7 T. K. Abbas, K. T. Rashid and Q. F. Alsalhy, NaY zeolite-polyethersulfone-modified membranes for the removal of cesium-137 from liquid radioactive waste, *Chem. Eng. Res. Des.*, 2022, **179**, 535–548. https://linkinghub.elsevier.com/retrieve/pii/S0263876222000557.
8 L. Guan and B. Wu, Membrane fouling of pressure retarded osmosis with CO2-captured alkali solutions as draw solutions, *Sch. Talk.*, 2023, **5**, 100146. https://linkinghub.elsevier.com/retrieve/pii/S277256932300021X.
9 W. K. Al-Musawy, M. H. Al-Furaiji and Q. F. Alsalhy, Synthesis and characterization of PVC-TFC hollow fibers for forward osmosis application, *J. Appl. Polym. Sci.*, 2021, **138**(35), 1–5.
10 M. Zhou, J. Chen, S. Yu, B. Chen, C. Chen, L. Shen, *et al.*, The coupling of persulfate activation and membrane separation for the effective pollutant degradation and membrane fouling alleviation, *Chem. Eng. J.*, 2023, **451**, 139009. https://linkinghub.elsevier.com/retrieve/pii/S1385894722044886.
11 S. T. Abdul-Hussein, M. H. Al-Furaiji, H. Meskher, D. Ghernaout, M. Fal, A. M. ALotaibi, *et al.*, Prospects of forward osmosis-based membranes for seawater mining: Economic analysis, limitations and opportunities, *Desalination*, 2024, **579**, 117477. https://linkinghub.elsevier.com/retrieve/pii/S0011916424001887.
12 T. W. Abood, K. M. Shabeeb, A. B. Alzubaydi, H. Meskher, A. K. Lafta, R. A. Al-Juboori, *et al.*, MXene-based pressure driven membranes for wastewater treatment: A critical review, *Desalin. Water Treat.*, 2024, **320**, 100594. https://linkinghub.elsevier.com/retrieve/pii/S1944398624006957.
13 E. S. Awad, T. M. Sabirova, N. A. Tretyakova, Q. F. Alsalhy, A. Figoli and I. K. Salih, A mini-review of enhancing ultrafiltration membranes (Uf) for wastewater treatment: Performance and stability, *ChemEngineering*, 2021, **5**(3), 1–27.
14 C. Sun and X. Feng, Enhancing the performance of PVDF membranes by hydrophilic surface modification via amine treatment, *Sep. Purif. Technol.*, 2017, **185**, 94–102. https://linkinghub.elsevier.com/retrieve/pii/S1383586616328210.
15 R. Kumar and A. F. Ismail, Fouling control on microfiltration/ultrafiltration membranes: Effects of morphology, hydrophilicity, and charge, *J. Appl. Polym. Sci.*, 2015, **132**(21), 1–20.
16 M. J. Park, R. R. Gonzales, A. Abdel-Wahab, S. Phuntsho and H. K. Shon, Hydrophilic polyvinyl alcohol coating on hydrophobic electrospun nanofiber membrane for high performance thin film composite forward osmosis membrane, *Desalination*, 2018, **426**, 50–59. https://linkinghub.elsevier.com/retrieve/pii/S0011916417322245.
17 T. A. Otitoju, A. L. Ahmad and B. S. Ooi, Recent advances in hydrophilic modification and performance of polyethersulfone (PES) membrane via additive blending, *RSC Adv.*, 2018, **8**(40), 22710–22728. http://xlink.rsc.org/?DOI=C8RA03296C.
18 N. H. Ismail, W. N. W. Salleh, A. F. Ismail, H. Hasbullah, N. Yusof, F. Aziz, *et al.*, Hydrophilic polymer-based membrane for oily wastewater treatment: A review, *Sep. Purif. Technol.*, 2020, **233**, 116007. https://linkinghub.elsevier.com/retrieve/pii/S1383586618339741.
19 A. L. Ahmad, A. A. Abdulkarim, B. S. Ooi and S. Ismail, Recent development in additives modifications of polyethersulfone membrane for flux enhancement, *Chem. Eng. J.*, 2013, **223**, 246–267. https://linkinghub.elsevier.com/retrieve/pii/S1385894713003240.
20 H. Meskher, T. Ragdi, A. K. Thakur, S. Ha, I. Khelfaoui, R. Sathyamurthy, *et al.*, A Review on CNTs-Based Electrochemical Sensors and Biosensors: Unique Properties and Potential Applications, *Crit. Rev. Anal. Chem.*, 2023, 1–24, DOI: 10.1080/10408347.2023.2171277.
21 E. Mahmoudi, L. Y. Ng, W. L. Ang, Y. T. Chung, R. Rohani and A. W. Mohammad, Enhancing Morphology and Separation Performance of Polyamide 6,6 Membranes By Minimal Incorporation of Silver Decorated Graphene Oxide Nanoparticles, *Sci. Rep.*, 2019, **9**(1), 1216. https://www.nature.com/articles/s41598-018-38060-x.
22 F. R. Mahdavi, B. Van der Bruggen, A. Verliefde and E. Cornelissen, A review of zeolite materials used in membranes for water purification: history, applications, challenges and future trends, *J. Chem. Technol. Biotechnol.*, 2022, **97**(3), 575–596, DOI: 10.1002/jctb.6963.
23 M. A. Tooma, T. S. Najim, Q. F. Alsalhy, T. Marino, A. Criscuoli, L. Giorno, *et al.*, Modification of polyvinyl chloride (PVC) membrane for vacuum membrane distillation (VMD) application, *Desalination*, 2015, **373**, 58–70. https://linkinghub.elsevier.com/retrieve/pii/S0011916415300163.
24 M. S. Rahaman, H. Thérien-Aubin, M. Ben-Sasson, C. K. Ober, M. Nielsen and M. Elimelech, Control of biofouling on reverse osmosis polyamide membranes modified with biocidal nanoparticles and antifouling polymer brushes, *J. Mater. Chem. B*, 2014, **2**(12), 1724. http://xlink.rsc.org/?DOI=c3tb21681k.
25 P. Daraei, S. S. Madaeni, N. Ghaemi, M. A. Khadivi, B. Astinchap and R. Moradian, Enhancing antifouling capability of PES membrane via mixing with various types of polymer modified multi-walled carbon nanotube, *J. Membr. Sci.*, 2013, **444**, 184–191. https://linkinghub.elsevier.com/retrieve/pii/S0376738813004079.
26 S. S. Hussein, S. S. Ibrahim, M. A. Toma, Q. F. Alsalhy and E. Drioli, Novel chemical modification of polyvinyl chloride membrane by free radical graft copolymerization for direct contact membrane distillation (DCMD) application, *J. Membr. Sci.*, 2020, **611**, 118266. https://linkinghub.elsevier.com/retrieve/pii/S0376738820308449.
27 T. Ahmad and C. Guria, Progress in the modification of polyvinyl chloride (PVC) membranes: A performance review for wastewater treatment, *J. Water Process Eng.*, 2022, **45**, 102466. https://linkinghub.elsevier.com/retrieve/pii/S2214714421005535.
28 A. J. Sadiq, E. S. Awad, K. M. Shabeeb, B. I. Khalil, S. M. Al-Jubouri, T. M. Sabirova, *et al.*, Comparative study of

embedded functionalised MWCNTs and GO in Ultrafiltration (UF) PVC membrane: Interaction mechanisms and performance, *Int. J. Environ. Anal. Chem.*, 2023, **103**(2), 415–436.

29 N. T. Thanh Truc, C.-H. Lee, B.-K. Lee and S. R. Mallampati, Development of hydrophobicity and selective separation of hazardous chlorinated plastics by mild heat treatment after PAC coating and froth flotation, *J. Hazard. Mater.*, 2017, **321**, 193–202. https://linkinghub.elsevier.com/retrieve/pii/S0304389416308172.

30 Q. F. Alsalhy, F. H. Al-Ani, A. E. Al-Najar and S. I. A. Jabuk, A study of the effect of embedding ZnO-NPs on PVC membrane performance use in actual hospital wastewater treatment by membrane bioreactor, *Chem. Process Eng.*, 2018, **130**, 262–274. https://linkinghub.elsevier.com/retrieve/pii/S0255270117311108.

31 N. F. H. Ismail, T. M. Chai, R. Daik and R. Othaman, Epoxidised natural rubber (ENR)/polyvinyl chloride (PVC)/silica (SiO2) membrane for treating palm oil mill effluents (POME), *Plast., Rubber Compos.*, 2020, **49**(3), 134–140, DOI: 10.1080/14658011.2020.1718323.

32 Y. M. Kim, S. H. Choi, H. C. Lee, M. Z. Hong, K. Kim and H.-I. Lee, Organic–inorganic composite membranes as addition of SiO2 for high temperature-operation in polymer electrolyte membrane fuel cells (PEMFCs), *Electrochim. Acta*, 2004, **49**(26), 4787–4796. https://linkinghub.elsevier.com/retrieve/pii/S0013468604005626.

33 H. Mahdavi, N. Zeinalipour, M. A. Kerachian and A. A. Heidari, Preparation of high-performance PVDF mixed matrix membranes incorporated with PVDF-g-PMMA copolymer and GO@SiO2 nanoparticles for dye rejection applications, *J. Water Process Eng.*, 2022, **46**, 102560. https://linkinghub.elsevier.com/retrieve/pii/S2214714422000034.

34 M. Hicham, A. Fethi, S. Ha and B. Khaldoun, Antifouling double layers of functionalized-multi-walled carbon nanotubes coated ZnO for sensitive and selective electrochemical detection of catechol, *Fullerenes, Nanotub. Carbon Nanostruct.*, 2022, **30**(3), 334–347, DOI: 10.1080/1536383X.2021.1940150.

35 D. D. Al-Araji, F. H. Al-Ani and Q. F. Alsalhy, Modification of polyethersulfone membranes by Polyethyleneimine (PEI) grafted Silica nanoparticles and their application for textile wastewater treatment, *Environ. Technol.*, 2022, 1–17.

36 Z. Yu, X. Liu, F. Zhao, X. Liang and Y. Tian, Fabrication of a low-cost nano-SiO 2/PVC composite ultrafiltration membrane and its antifouling performance, *J. Appl. Polym. Sci.*, 2015, **132**(2), DOI: 10.1002/app.41267.

37 S. Saberi, A. A. Shamsabadi, M. Shahrooz, M. Sadeghi and M. Soroush, Improving the Transport and Antifouling Properties of Poly(vinyl chloride) Hollow-Fiber Ultrafiltration Membranes by Incorporating Silica Nanoparticles, *ACS Omega*, 2018, **3**(12), 17439–17446, DOI: 10.1021/acsomega.8b02211.

38 R. Stanley and a S. Nesaraj, Effect of Surfactants on the Wet Chemical Synthesis of Silica Nanoparticles, *Int. J. Appl. Sci. Eng.*, 2014, 9–21.

39 H. M. Mezher, H. Adeli and Q. F. Alsalhy, Novel ZnO-Modified Polyethersulfone Nanocomposite Membranes for Nanofiltration of Concentrated Textile Wastewater, *Water, Air, Soil Pollut.*, 2024, **235**(2), 138.

40 J. Dalmijn, J. Glüge, M. Scheringer and I. T. Cousins, Emission inventory of PFASs and other fluorinated organic substances for the fluoropolymer production industry in Europe, *Environ. Sci.:Processes Impacts*, 2024, **26**(2), 269–287.

41 C. M. Hansen, *Hansen Solubility Parameters: a User's Handbook*, CRC press, 2007.

42 W. Xie, T. Li, A. Tiraferri, E. Drioli, A. Figoli, J. C. Crittenden, *et al.*, Toward the Next Generation of Sustainable Membranes from Green Chemistry Principles, *ACS Sustain. Chem. Eng.*, 2021, **9**(1), 50–75, DOI: 10.1021/acssuschemeng.0c07119.

43 D. M. Al-Ani, F. H. Al-Ani, Q. F. Alsalhy and S. S. Ibrahim, Preparation and characterization of ultrafiltration membranes from PPSU-PES polymer blend for dye removal, *Chem. Eng. Commun.*, 2021, **208**(1), 41–59, DOI: 10.1080/00986445.2019.1683546.

44 Z. Xu, J. Zhang, M. Shan, Y. Li, B. Li, J. Niu, *et al.*, Organosilane-functionalized graphene oxide for enhanced antifouling and mechanical properties of polyvinylidene fluoride ultrafiltration membranes, *J. Membr. Sci.*, 2014, **458**, 1–13. https://linkinghub.elsevier.com/retrieve/pii/S0376738814000635.

45 D. Al-Araji, F. Al-Ani and Q. Alsalhy, The permeation and Separation Characteristics of Polymeric Membranes Incorporated with Nanoparticles for Dye Removal and Interaction Mechanisms between Polymer and Nanoparticles: A Mini Review, *J. Eng. Technol.*, 2022, **40**(11), 1399–1411. https://etj.uotechnology.edu.iq/article_174970.html.

46 R. R. Abdullah, M. K. Shabeeb, B. A. Alzubaydi, A. Figoli, A. Criscuoli, E. Drioli, *et al.*, Characterization of the Efficiency of Photo-Catalytic Ultrafiltation PES Membrane Modified with Tungsten Oxide in the Removal of Tinzaparin Sodium, *J. Eng. Technol.*, 2022, **40**(12), 1–10. https://etj.uotechnology.edu.iq/article_174998.html.

47 L. S. Clesceri, E. W. Rice, and A. E. Greenberg, *Standard Methods for the Examination of Water and Wastewater*, Am Public Heal Assoc, Washington, DC, 22nd edn, 2012.

48 R. R. Abdullah, K. M. Shabeed, A. B. Alzubaydi and Q. F. Alsalhy, Novel photocatalytic polyether sulphone ultrafiltration (UF) membrane reinforced with oxygen-deficient Tungsten Oxide (WO2.89) for Congo red dye removal, *Chem. Eng. Res. Des.*, 2022, **177**, 526–540. https://linkinghub.elsevier.com/retrieve/pii/S0263876221004767.

49 N. Reddeppa, A. K. Sharma, V. V. R. N. Rao and W. Chen, AC conduction mechanism and battery discharge characteristics of (PVC/PEO) polyblend films complexed with potassium chloride, *Measurement*, 2014, **47**, 33–41.

50 H. Yu, X. Zhang, Y. Zhang, J. Liu and H. Zhang, Development of a hydrophilic PES ultrafiltration membrane containing SiO2@ N-Halamine nanoparticles with both organic antifouling and antibacterial properties, *Desalination*, 2013, **326**, 69–76.

51 P. Wu, X. Guo, Y. Zhong, C. Liu, S. Chen, Y. Wang, *et al.*, How the Si–O–Si Covalent Bond Interface Affects the Electrochemical Performance of the Silicon Anode, *ACS Appl. Energy Mater.*, 2022, **5**(5), 6373–6382, DOI: **10.1021/acsaem.2c00747**.

52 L. Y. Ng, A. W. Mohammad, C. P. Leo and N. Hilal, Polymeric membranes incorporated with metal/metal oxide nanoparticles: A comprehensive review, *Desalination*, 2013, **308**, 15–33. **https://linkinghub.elsevier.com/retrieve/pii/S0011916410008611**.

53 D. Jha, A. G. Kusne, R. Al-Bahrani, N. Nguyen, W. Liao, A. Choudhary, *et al.*, Peak Area Detection Network for Directly Learning Phase Regions from Raw X-ray Diffraction Patterns, in *2019 International Joint Conference on Neural Networks (IJCNN)*, IEEE, 2019, pp. 1–8, **https://ieeexplore.ieee.org/document/8852096/**.

54 H. Wang, X. Li, X. Feng, Y. Liu, W. Kang, X. Xu, *et al.*, Novel proton-conductive nanochannel membranes with modified SiO2 nanospheres for direct methanol fuel cells, *J. Solid State Electrochem.*, 2018, **22**(11), 3475–3484, DOI: **10.1007/s10008-018-4057-1**.

55 A. M. Abdelghany, M. S. Meikhail and R. Hamdy, Enrichment of poly vinyl chloride (PVC) biological uses through sodium chloride filler, density functional theory (DFT) supported experimental study, *J. Adv. Phys.*, 2018, **14**(3), 5682–5692.

56 A. W. Mohammad, N. Hilal, Y. P. Lim, I. N. H. M. Amin and R. Raslan, Atomic force microscopy as a tool for asymmetric polymeric membrane characterization, *Sains Malays.*, 2011, **40**(3), 237–244.

57 X. Cao, J. Ma, X. Shi and Z. Ren, Effect of TiO2 nanoparticle size on the performance of PVDF membrane, *Appl. Surf. Sci.*, 2006, **253**(4), 2003–2010.

58 C. Mahmoudi, E. Demirel and Y. Chen, Investigation of characteristic and performance of polyvinyl chloride ultrafiltration membranes modified with silica-oriented multi walled carbon nanotubes, *J. Appl. Polym. Sci.*, 2020, **137**(45), 49397.

59 M. R. S. Kebria, M. Jahanshahi and A. Rahimpour, SiO_2 modified polyethyleneimine-based nanofiltration membranes for dye removal from aqueous and organic solutions, *Desalination*, 2015, **367**, 255–264, DOI: **10.1016/j.desal.2015.04.017**.

60 Q. Zheng and C. Lü, Size Effects of Surface Roughness to Superhydrophobicity, *Procedia IUTAM*, 2014, **10**, 462–475. **https://linkinghub.elsevier.com/retrieve/pii/S221098381400042X**.

61 D. Johnson and N. Hilal, Polymer membranes–Fractal characteristics and determination of roughness scaling exponents, *J. Membr. Sci.*, 2019, **570**, 9–22.

62 Q. Alsalhy, S. Algebory, G. M. Alwan, S. Simone, A. Figoli and E. Drioli, Hollow fiber ultrafiltration membranes from poly(vinyl chloride): Preparation, morphologies, and properties, *Sep. Sci. Technol.*, 2011, **46**(14), 2199–2210.

63 S. Darvishmanesh, J. C. Jansen, F. Tasselli, E. Tocci, P. Luis, J. Degrève, *et al.*, Novel polyphenylsulfone membrane for potential use in solvent nanofiltration, *J. Membr. Sci.*, 2011, **379**(1–2), 60–68.

64 T. Kumar Dey, J. Hou, M. Sillanpää and B. Kumar Pramanik, Metal-organic framework membrane for waterborne micro/nanoplastics treatment, *Chem. Eng. J.*, 2023, **474**, 145715. **https://linkinghub.elsevier.com/retrieve/pii/S1385894723044467**.

65 L. Zhou, Y. Fang, J. Ye, M. Chen, H. Yang and Z. Xu, Cross-section and pore size regulation of hydroxyurea-modified polyacrylonitrile membrane by NH2-CNT and Si(OEt)4 filler and heat treatment for dye removal application at medium temperature, *Sep. Purif. Technol.*, 2023, **323**, 124430. **https://linkinghub.elsevier.com/retrieve/pii/S1383586623013382**.

66 F. H. Al-Ani, Q. F. Alsalhy, R. S. Raheem, K. T. Rashid and A. Figoli, Experimental investigation of the effect of implanting tio2-nps on pvc for long-term uf membrane performance to treat refinery wastewater, *Membranes*, 2020, **10**(4), 77.

67 D. A. H. Al-timimi, Q. F. Alsalhy, A. A. Abdulrazak and E. Drioli, Novel polyether sulfone/polyethylenimine grafted nano-silica nanocomposite membranes : Interaction mechanism and ultrafiltration performance, *J. Membr. Sci.*, 2022, **659**, 120784, DOI: **10.1016/j.memsci.2022.120784**.

68 S. M. Mousavi, S. Raveshiyan, Y. Amini and A. Zadhoush, A critical review with emphasis on the rheological behavior and properties of polymer solutions and their role in membrane formation, morphology, and performance, *Adv. Colloid Interface Sci.*, 2023, **319**, 102986. **https://linkinghub.elsevier.com/retrieve/pii/S0001868623001537**.

69 T. Kumar Dey, L. Fan, M. Bhuiyan and B. Kumar Pramanik, Evaluating the performance of the metal organic framework-based ultrafiltration membrane for nanoplastics removal, *Sep. Purif. Technol.*, 2025, **353**, 128658. **https://linkinghub.elsevier.com/retrieve/pii/S1383586624023979**.

70 Y. A. Jarma, J. Thompson, B. M. Khan and Y. Cohen, Field Evaluation of UF Filtration Pretreatment Impact on RO Membrane Scaling, *Water*, 2023, **15**(5), 847.

71 A. Siddique, A. A. Yaqoob, M. A. Mirza, A. Kanwal, M. N. M. Ibrahim and A. Ahmad, Potential use of ultrafiltration (UF) membrane for remediation of metal contaminants, in *Emerging Techniques for Treatment of Toxic Metals from Wastewater*, Elsevier, 2023, pp. 341–364.

72 M. Zielińska and M. Galik, Use of Ceramic Membranes in a Membrane Filtration Supported by Coagulation for the Treatment of Dairy Wastewater, *Water, Air, Soil Pollut.*, 2017, **228**(5), 173, DOI: **10.1007/s11270-017-3365-x**.

73 Y. Zhu and W. Yue, Hydraulic tortuosity of porous media: comparison of different modeling methods, *J. Geophys. Eng.*, 2024, **21**(3), 833–843. **https://academic.oup.com/jge/article/21/3/833/7644350**.

74 C. D. Peters, T. Rantissi, V. Gitis and N. P. Hankins, Retention of natural organic matter by ultrafiltration and the mitigation of membrane fouling through pre-treatment, membrane enhancement, and cleaning – A review, *J. Water Process Eng.*, 2021, **44**, 102374. **https://linkinghub.elsevier.com/retrieve/pii/S221471442100461X**.

75 S. Sharma, S. Gupta, S. Kaur, D. Kumar, P. Banerjee and A. K. Nadda, *Polymeric Membranes for Water Treatment*, 2023, pp. 1–21. DOI: **10.1007/978-981-19-9176-9_1**.

76 F. Suárez, M. B. del Río and J. E. Aravena, Water Flux Prediction in Direct Contact Membrane Distillation Subject to Inorganic Fouling, *Membranes*, 2022, **12**(2), 157. **https://www.mdpi.com/2077-0375/12/2/157**.

77 A. A. Jimoh, E. Booysen, L. van Zyl and M. Trindade, Do biosurfactants as anti-biofilm agents have a future in industrial water systems?, *Front. Bioeng. Biotechnol.*, 2023, **11**, 1–17.

78 D. Uçar, Membrane processes for the reuse of car washing wastewater, *J. Water Reuse Desalin.*, 2018, **8**(2), 169–175.

79 F. S. Kamelian, S. M. Mousavi, A. Ahmadpour and V. Ghaffarian, Preparation of acrylonitrile-butadiene-styrene membrane: Investigation of solvent/nonsolvent type and additive concentration, *Korean J. Chem. Eng.*, 2014, **31**(8), 1399–1404.

80 A. Rahimpour, B. Rajaeian, A. Hosienzadeh, S. S. Madaeni and F. Ghoreishi, Treatment of oily wastewater produced by washing of gasoline reserving tanks using self-made and commercial nanofiltration membranes, *Desalination*, 2011, **265**(1–3), 190–198.

81 S. A. Kiran, G. Arthanareeswaran, Y. L. Thuyavan and A. F. Ismail, Influence of bentonite in polymer membranes for effective treatment of car wash effluent to protect the ecosystem, *Ecotoxicol. Environ. Saf.*, 2015, **121**, 186–192.

82 T. D. Kusworo, H. Al-Aziz and D. P. Utomo, UV irradiation and PEG additive effects on PES hybrid membranes performance in rubber industry wastewater treatment, *AIP Conf. Proc.*, 2020, **2197**, 1–6, **https://pubs.aip.org/aip/acp/article/782759**.

83 V. Vatanpour, M. Hazrati, M. Sheydaei and A. Dehqan, Investigation of using UV/H2O2 pre-treatment process on filterability and fouling reduction of PVDF/TiO2 nanocomposite ultrafiltration membrane, *Chem. Eng. Process.*, 2022, **170**, 108677.